AD-A092 626 FRAUNHOFER-GESELLSCHAFT FREIBURG (GERMANY F R) INST--ETC F/G 20/12
DYNAMIC PROPERTIES OF INTERFACE STATES IN MOS-STRUCTURES.(U)
MAR 80 E KLAUSMANN, A GOETZBERGER DAJA37-79-C-0547

UNCLASSIFIED NL

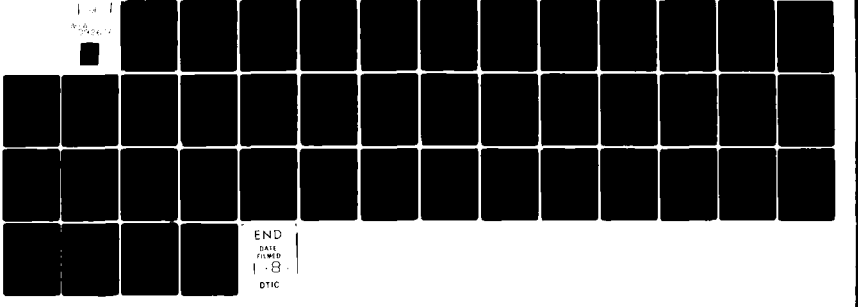

END
DATE FILMED
1-8
DTIC

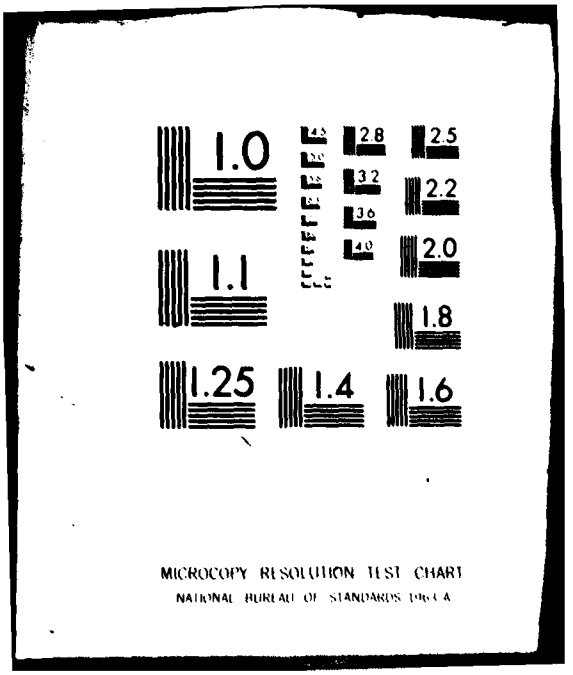
1.0
1.1
1.25
1.4
1.6
2.8
3.2
3.6
4.0
2.5
2.2
2.0
1.8
MICROCOPY RESOLUTION TEST CHART
NATIONAL BUREAU OF STANDARDS 1963 A

AD

DYNAMIC PROPERTIES OF INTERFACE STATES IN MOS-STRUCTURES

Final Technical Report

by

E. Klausmann and A. Goetzberger

March 1980

EUROPEAN RESEARCH OFFICE

United States Army

London England

GRANT NUMBER DAJA37-79-C-0547

Fraunhofer-Institut für Angewandte Festkörperphysik
Freiburg/W.-Germany

AD

DYNAMIC PROPERTIES OF INTERFACE STATES IN MOS-STRUCTURES

Final Technical Report

by

E. Klausmann and A. Goetzberger

March 1980

EUROPEAN RESEARCH OFFICE

United States Army

London England

GRANT NUMBER DAJA37-79-C-0547

Fraunhofer-Institut für Angewandte Festkörperphysik
Freiburg/W.-Germany

UNCLASSIFIED

SECURITY CLASSIFICATION OF THIS PAGE (When Data Entered)

R&D 2722

REPORT DOCUMENTATION PAGE		READ INSTRUCTIONS BEFORE COMPLETING FORM
1. REPORT NUMBER	2. GOVT ACCESSION NO. AD-A093 626	3. RECIPIENT'S CATALOG NUMBER
4. TITLE (and Subtitle) Dynamic Properties of Interface States in MOS-Structures		5. TYPE OF REPORT & PERIOD COVERED Final Technical Report Sep 79 - May 80
		6. PERFORMING ORG. REPORT NUMBER
7. AUTHOR(s) E. Klausmann and A. Goetzberger		8. CONTRACT OR GRANT NUMBER(s) DAJA37-79-C-0547
9. PERFORMING ORGANIZATION NAME AND ADDRESS Fraunhofer-Institut für Angewandte Festkörperphysik Freiburg West Germany		10. PROGRAM ELEMENT, PROJECT, TASK AREA & WORK UNIT NUMBERS 61102A 1T161102BH57-03
11. CONTROLLING OFFICE NAME AND ADDRESS USARDSG-UK Box 65 FPO NY 09510		12. REPORT DATE March 80
		13. NUMBER OF PAGES 21
14. MONITORING AGENCY NAME & ADDRESS(if different from Controlling Office)		15. SECURITY CLASS. (of this report) Unclassified
		15a. DECLASSIFICATION/DOWNGRADING SCHEDULE

16. DISTRIBUTION STATEMENT (of this Report)

Approved for Public Release; distribution unlimited

17. DISTRIBUTION STATEMENT (of the abstract entered in Block 20, if different from Report)

18. SUPPLEMENTARY NOTES

19. KEY WORDS (Continue on reverse side if necessary and identify by block number)

Semiconductors
Surface States
Deep Levels

20. ABSTRACT (Continue on reverse side if necessary and identify by block number)

With the CC-DLTS (= constant capacitance deep level transient spectroscopy) method the energy distribution of the interface state density and the capture cross sections of MOS structures can be determined. A new evaluation procedure for this method was developed.

The procedure used hitherto was based on rather restrictive assumptions and therefore provided results of lesser reliability. The new procedure requires →

DD FORM 1 JAN 73 1473 EDITION OF 1 NOV 65 IS OBSOLETE

UNCLASSIFIED

SECURITY CLASSIFICATION OF THIS PAGE (When Data Entered)

20. Contd.

more experimental data than the previous one, because one had overlooked that the basic equations possess more than one solution. The limits of the new procedure are outlined.

A full evaluation for the energy distribution of both the interface state density and the capture cross sections is in the reach of today's instrumental means if $N_{ss} \gtrsim 10^{10} V^{-1} cm^{-2}$. The previous method has a semi-quantitative character. Though it yields interface state densities down to $10^{9} V^{-1} cm^{-2}$, it does not permit evaluation of capture cross sections and energy distribution.

An experimental comparison of the CC-DLTS and conductance methods is presented.

Summary

With the CC-DLTS (= constant capacitance deep level transient spectroscopy) method the energy distribution of the interface state density and the capture cross sections of MOS structures can be determined. A new evaluation procedure for this method was developed.

The procedure used hitherto was based on rather restrictive assumptions and therefore provided results of lesser reliability. The new procedure requires more experimental data than the previous one, because one had overlooked that the basic equations possess more than one solution. The limits of the new procedure are outlined.

A full evaluation for the energy distribution of both the interface state density and the capture cross sections is in the reach of to-day's instrumental means if $N_{ss} \geq 10^{10}\ V^{-1}cm^{-2}$. The previous method has a semi-quantitative character. Though it yields interface state densities down to $10^{9}\ V^{-1}cm^{-2}$, it does not permit evaluation of capture cross sections and energy distribution.

An experimental comparison of the CC-DLTS and conductance methods is presented.

Table of Contents

Appendix

Introduction

As pointed out in the last "Final Technical Report" (January 1979) we observed an inconsistency in the results obtained by the CC-DLTS method. The results did not agree with the results of the conductance method, and they showed some peculiarities. At first it seemed that they might only be explained by far-fetched assumptions. We could show, however, that this inconsistency was likely to be caused by an insufficient mathematical approximation of the basic equations. We conjectured that the dependence of the capture cross sections on energy was unduly neglected. During the past year this problem was investigated in more detail, and we found that the conjecture proved to be true. A new evaluation procedure for the CC-DLTS method was then developed. The results of this new evaluation were compared with the results of the conductance method. The results of both methods have agreed well, and the peculiarities previously found have disappeared.

A paper about the new method was presented at the INFOS 79-conference at Durham. An article was published in the conference proceedings /1/. The new method and the most important results have been described there. That article is reprinted in Appendix A of this report. We will therefore dispense with another description of the new method. Because of the limited space in the conference proceedings some points, however, have had to be cut down or omitted. The points which were left out there and some results which were obtained in the meantime will now be given in more detail in the following.

If not otherwise mentioned, the experimental examples in this report refer to the same n-type MOS sample already described in Appendix A.

I. A comparison of the old and the new evaluation method

Although the former evaluation is a crude approximation, it is nevertheless worthwhile looking at the differences between the two methods: In case the correlation signal data are near the limit to be measured with sufficient accuracy, one may still obtain useful semiquantitative values for the interface state density N_{ss} (but not for the capture cross sections σ) with an evaluation according to the previous method.

Therefore it is advisable to be familiar with the errors that can be introduced with such an evaluation.

The main difference between the two methods is the different treatment of the derivative $d \ln \sigma / dE$. The equations A.9 and A.10[+)] hold for both methods:

[+)] The equations and figures denoted with A refer to Appendix A.

$$(1) \qquad N_{ss}(E_o) = \frac{C_{ox}}{A} \quad \Delta V_G(t_i, T) \quad \frac{1}{kT \ln 2} \quad \left(1 + kT \frac{d \ln \sigma}{dE}\right)$$

In the old method the term with the derivative $d \ln \sigma / dE$ is considered to be only a correction term which is neglected. Indeed, rarely does it exceed a value of more than 30 %. Hence, both methods give nearly the same results for the interface state density N_{ss}.

One has to pay attention when evaluating according to the old method that the left side of eq. (1) has to be first considered to be a function of T. Not until the second step of the evaluation is done is the temperature T put in relation to the energy E_o. The second step, however, is faulty as shown in the end of this paragraph. The analysis therefore has to be stopped after calculating only $N_{ss}(T)$. One knows, however, that the low temperatures are related to energies near the majority carrier band edge and temperatures near the room temperature mean midgap energies.

One must bear in mind, that occasionally this inaccurate evaluation may produce spurious structures, e.g. peaks, into the N_{ss}-curves. This occurs, if $d \ln \sigma / dE$ changes rapidly within a small energy range. As this change is not taken into consideration when the correction term is neglected, this change then appears in the N_{ss}-curve.

The evaluation of the capture cross sections σ and the energy E according to the former method fails entirely. Although sometimes the results of the former and the new methods in respect to $\sigma(E)$ happen to agree fairly well, we have to state that such an agreement is only fortuitous: In the old method, where the derivative $d \ln \sigma / dE$ is neglected, the eq. A.9 and A.10 then are algebraic equations. Their solution is unambiguous.

In the improved method these equations are differential equations, and their solutions can be displayed in a family of curves (Fig. A.5).

As in the old method only $d \ln \sigma / dE$ is omitted, i.e.

$$(2) \qquad \frac{d \ln \sigma}{dE} = 0$$

but the remaining expressions are retained, the old solution is closely connected to the family of solutions of the new method: The old solution is represented by a trajectory to the family of curves. This trajectory interconnects the maximum and minimum values, i.e. all points of the family of curves where eq. (2) is valid.

An example is given in Fig. 1. The capture cross sections according to the old solution start for low temperatures (about 60 K) at the point marked by the single arrow. First the curve passes through the maxima, then it turns

back (at about 220 K) and passes through the minima and ends for high temperatures (about 260 K) at the point marked by the double arrow. Such retrograde curves are typical for the old solutions. Although the curve fits the points of the conductance measurements at low temperatures quite well, the agreement must be held only to be accidentally good. The mathematical construction of the old solution lacks the physical basis. Another evidence that the old method is faulty is given by putting the solution into the exact equation A.1. In Fig. 2 one can see that the input data are not reproduced by the former solution.

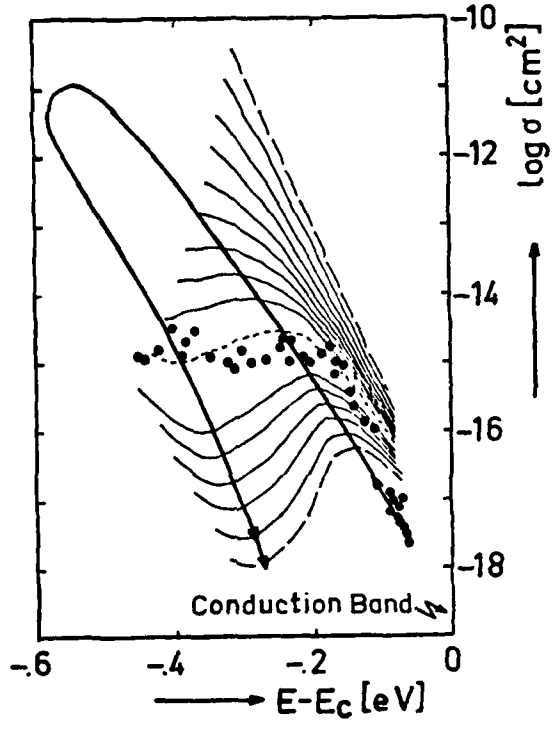

Fig. 1 Comparison of the former and the new evaluations. The method hitherto used yields for the capture cross section curve the trajectory through the maxima and minima of the family of curves obtained by the new evaluation (compare Fig. A.5).

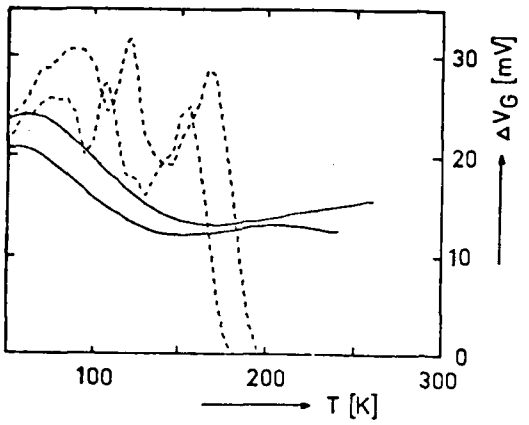

Fig. 2 Result of a check calculation. The solution of the old method was put into the exact integral for obtaining the correlation signals (eq. A.1). The measured correlation signals (solid curves) have not been reproduced by the calculated correlation signals (broken curves). The improvement achieved by the new evaluation can be assessed by a comparison with Fig. A.3 .

II. Supplementary comments about the determination of the integration constant

It is shown in Appendix A that the differential equation of the CC-DLTS method yields a family of solutions $N_{ss}(E, \sigma_o)$ and $\sigma(E, \sigma_o)$[+] . The different solutions are distinguished by the different initial values (integration constants) σ_o . The correlation signals calculated from each of these solutions can possess different behaviour in respect to temperature. This occurs in the case when the energy E_o is close to the Fermi level E_s (cf. Fig. A.1) and consequently the emission gets limited. For each solution this reduced emission comes into effect at a different temperature. The reduced emission is seen as a sharp drop of the correlation signal. An example is given in Fig. 3 a and b.

When the curves of Fig. 3 a had been calculated surface potential fluctuations were not taken into account. The actual conditions are therefore somewhat more complicated. In Fig. 4 one curve out of this family is corrected for surface potential fluctuations of various magnitudes.

[+] In this report we call one pair of functions $N_{ss}(E, \sigma_o)$, $\sigma(E, \sigma_o)$ one solution.

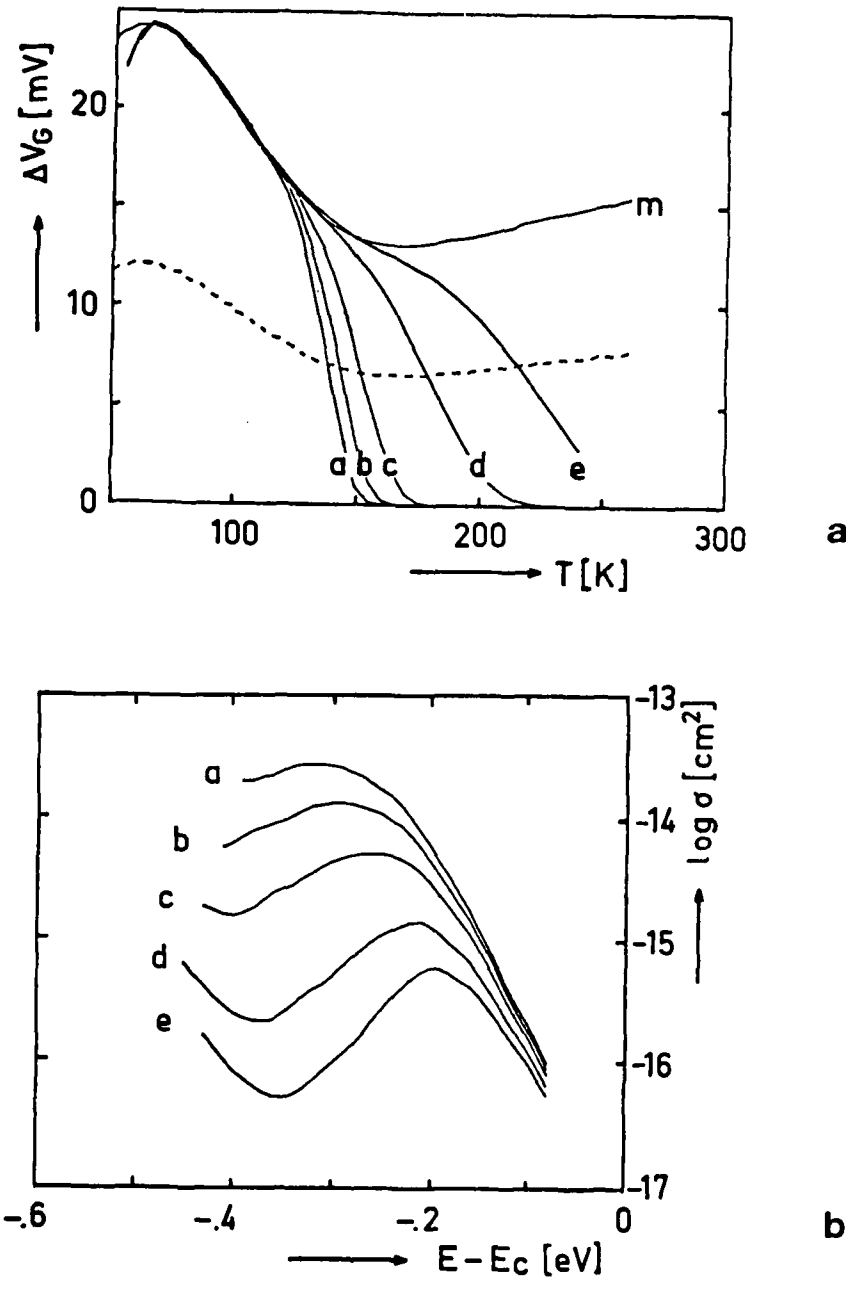

Fig. 3 Correlation signals in case the emission is limited by E_s. The correlation signals (Fig. 3a, a - e) are calculated with E_s = -0.4 eV and σ_g = 0. The curves refer to the different solutions of the differential equation, which are depicted in Fig. 3 b.
Curve m is the measured correlation signals with E_s = -0.5 eV. The dotted line is obtained from m by plotting half its value. The intersections of the dotted curve with the correlation signal curves are independent of variations in σ_g (cf. Fig. 4) The sampling times to all the curves were 2.5 ms/5 ms.

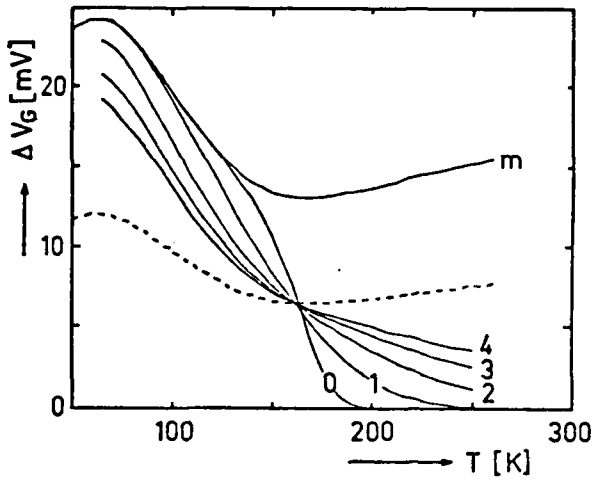

Fig. 4 Correlation signal in case the emission is limited by E_s and surface potential fluctuations are taken into account. One of the curves (0) belonging to the family of curves of Fig. 3 a is modified by taking surface potential fluctuations of different magnitudes (σ_g = 0, 1, 2, 3, 4 at 300 K) into account. All these curves intersect at a common point which has half the value of the correlation signal whose emission is not limited.
When calculating these curves it has been assumed that $\sigma_g \propto 1/T$.

These curves have been calculated according to eq. A.14. As can be seen from Fig. 4 there is a characteristic point, which is common to all the curves of different variances σ_g. This point is characterized by the decrease of the correlation signals to virtually half the value of the original one.

Therefore we can maintain as a rule for choosing the proper solution $N_{ss}(E)$ and $\sigma(E)$: First we have to record a correlation signal, the emission of which gets limited in a reasonable temperature region. Then we have to calculate correlation signals (for any σ_g, say $\sigma_g = 0$) pertinent to different solutions $N_{ss}(E, \sigma_o)$, $\sigma(E, \sigma_o)$. The criterion for the proper solution is the agreement of the temperature T_c where the calculated correlation signal has dropped to half of its original value, to the temperature T_m of the corresponding point of the measured curve. In a third step an adjustment of the variance σ_g can be attempted.

Attentive readers will notice a discrepancy between the curves of Fig. A.6 and Fig. 4 at low temperatures. A slight inaccuracy occurred in the description to Fig. A.6:

The curves of Fig. A.6 were calculated according to eq. A.14, but not - as stated in Appendix A - with $\sigma_g \propto 1/T$. We used a modified relation

$$\sigma_g \propto \frac{T}{T + T'} \qquad \text{with } T' = 100 \text{ K.}$$

This relation yielded a better fit of the calculated curve to the measured curve.

Such a modified relation can be justified. The proportionality between σ_g and $1/T$ is only a first order approximation. There is also a small dependence on the situation of the Fermi level E_s. In case E_s is moving towards the majority carrier band edge the variance σ_g decreases. Since with the CC-DLTS technique E_s indeed moves towards the conduction band edge when the temperature is lowered, the $1/T$-dependence of σ_g has to be mitigated. This modified relation has not impaired the conclusions drawn here or in Appendix A.

III. Error analysis

The main experimental errors are found in noise and drift of the correlation signals. In comparison to these errors the other errors involved in the measurement (e.g. oxide capacitance, surface potential, etc.) can be neglected. In order to come to an estimation of how strongly these errors influence the results the (2.5 ms - 5 ms)-correlation signal (curve B of Fig. A.3) was modified in ten different ways by a computer simulation. The deviations to the actual data have been 0.5 % on the average and 1 % at most.

The ten results are displayed in the Fig. 5 and 6. The curves of the capture cross sections intersect at a fitting point arbitrarily chosen on the curve which represents the best fit to the conductance measurements.

It must be taken into account that

- the errors mentioned above are somewhat too optimistically assessed
- the other correlation signal should also be varied in the same way
- the fitting point is also subjected to errors.

Therefore the actual error margin will be roughly given by the dotted lines.

To present numerical values: The error of the interface state density amounts to about 25 %, and the error of the capture cross sections is about an order of magnitude. In comparison the errors of the same sample according to the conductance method are smaller by about a factor 4.

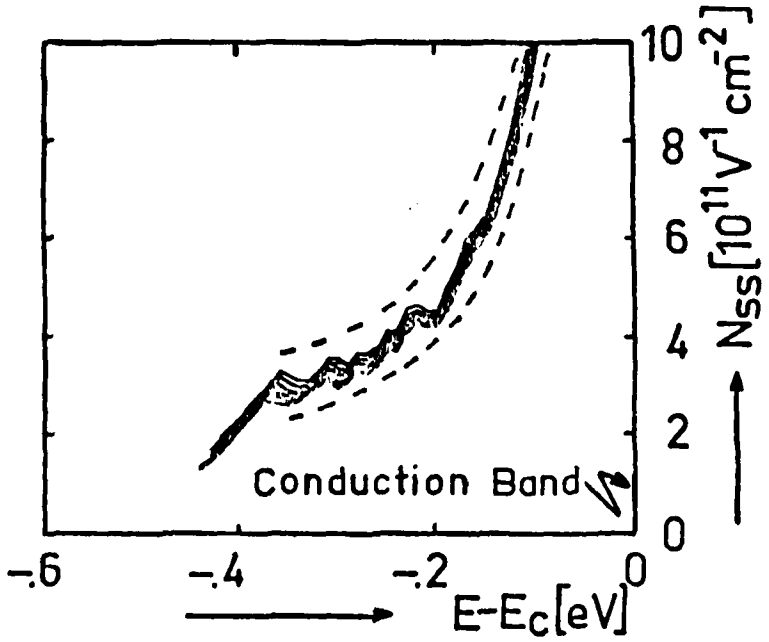

Fig. 5 Error analysis of the interface state density (cf. Fig. A.4). One of the correlation signals of Fig. A.3 was modified less than 1 % (0.5 % on the average) in ten different ways. As the experimental errors are greater, the dotted lines represent the real error margin.

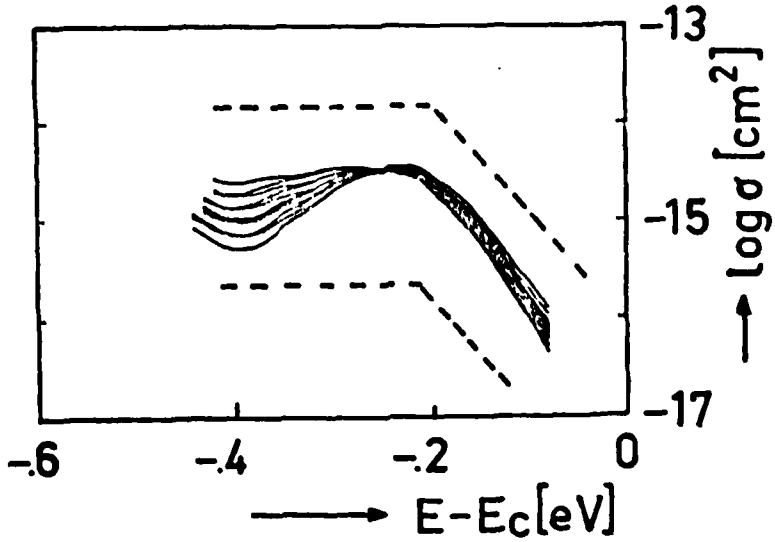

Fig. 6 Error analysis of the capture cross sections (cf. Fig. A.5).

It is still too early a stage of investigation as to supply a general error analysis of the CC-DLTS method. Surely the method is amenable to further improvement. Considering these results and complementing them by the findings of paragraph V (p-type sample) we may hope that a full evaluation for $N_{ss}(E)$ and $\sigma(E)$ will be achieved for $N_{ss} \gtrsim 10^{10}\ V^{-1}cm^{-2}$, if the equipment is improved. A reduced evaluation with respect to $N_{ss}(T)$ (cf. paragraph I) is possible for $N_{ss} \gtrsim 10^{9}\ V^{-1}cm^{-2}$ or perhaps even smaller values.

IV. CC-DLTS analysis of interfaces with different types of interface states

When deriving the evaluation method of Appendix A it has been presupposed that two (or more) types of interface states of the same energy with different capture cross sections must not be present in the interface. In Fig. 7 a - c and Fig. 8 a - c results are depicted if this requirement is violated.

The results of these figures have been obtained by a computer simulation. Two types of interface states have been assumed:

(i) The interface state density of one of the two types is continuously increasing towards the majority band edge. The capture cross sections are constant and amount to $10^{-15}\ cm^2$ (double-lined curves in Fig. 7 b and c).

(ii) The other type is confined to a small energy interval (dotted curve in Fig. 7 b) with a constant interface state density smaller by a factor of about 5 than that one of the continuous states. The capture cross sections are also constant and amount to $10^{-10}\ cm^2$ (dotted curve in Fig. 7 c).

With each of these data the correlation signals according to eq. A.1 have been calculated and then added up (Fig. 7 a). The effect of the "single-level"-state is just discernible in the correlation signals at about 150 K.

A formal evaluation according to the method of Appendix A yields the family of functions shown in Fig. 7 b and c (solid curves).

The modification of the correlation signals caused by the single level state deforms the capture cross section curves conspicuously. The same humps then again turn up in the curves of the interface state density (Fig. 7 b). Similar to the deformations of the N_{ss}-curves described in paragraph I, the deviations of the N_{ss}- curves are either positive or negative depending on the sign of the derivative of the σ-curve.

The contents of Fig. 8 a - c are the same as of Fig. 7, except a larger interface state density of the single level state has been assumed. Several

curves are split. This occurred because the numerical values of some auxiliary variables got outside the available range of the computer used.

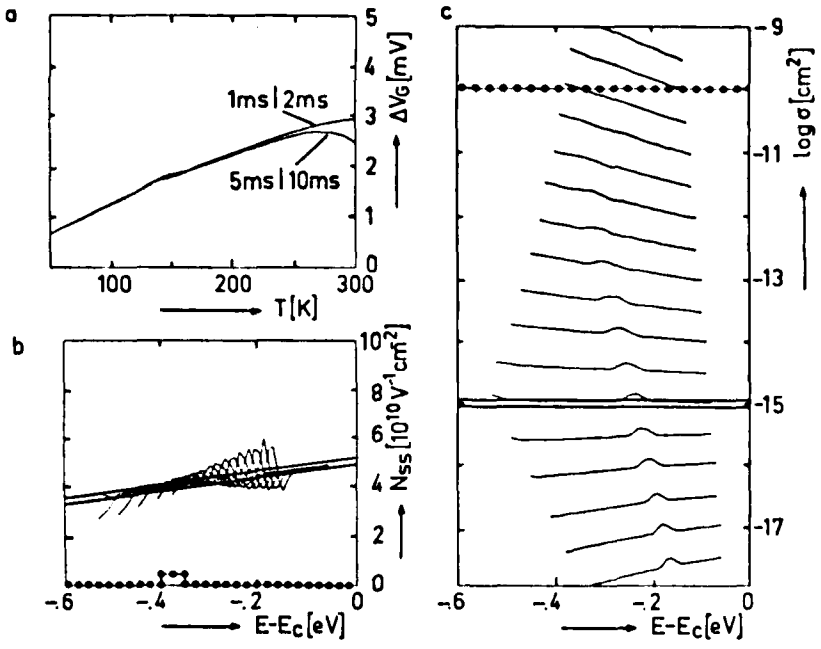

Fig. 7 CC-DLTS evaluation of samples with two types of interface states.
It has been stated in Appendix A that the suggested CC-DLTS evaluation fails if two (or more) types of interface states are involved. These figures show the result of a computer simulation. It has been assumed, that two types of interface states are simultanously present: (i) continuous states (double lines in Fig. b and c), (ii) a "single level" state (dotted lines in Fig. b and c). With these data as initial values the correlation signals (Fig. a) were calculated according to eq. A.1. Then the evaluation method of Appendix A was applied to these computed correlation signals. The results are displayed in Fig. b and c. They show what has already been stated, that the purview is transgressed within which the CC-DLTS evaluation according to Appendix A can be employed.

It has not been shown in the figures that by inserting the solutions into the correlation integral (eq. A. 1) the test calculation reproduces the starting correlation signals rather badly.

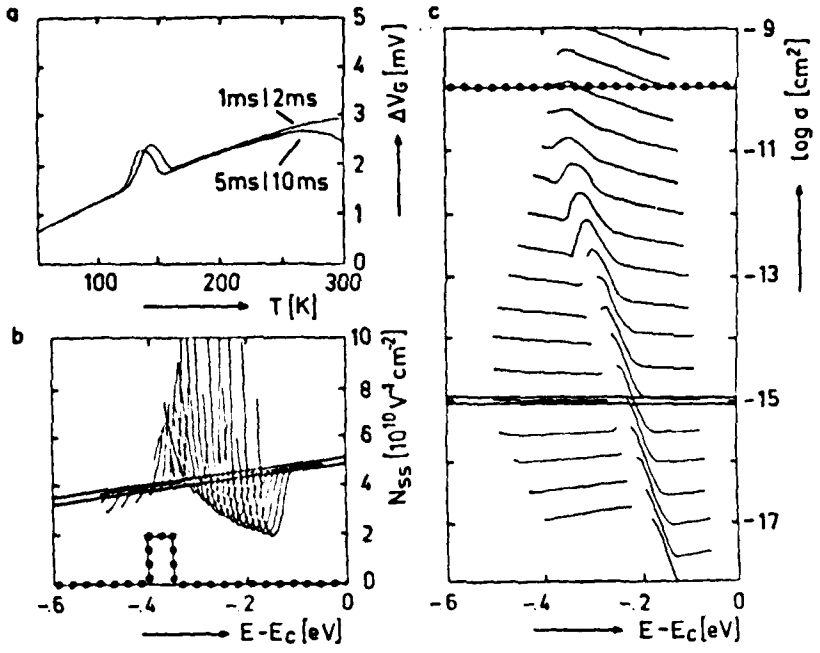

Fig. 8 CC-DLTS evaluation of samples with two types of interface states.
The contents are the same as in Fig. 7, except the density of the "single level" state is increased.

In conclusion we have to state: If more than one type of interface state is suspected to be present, then the results of the evaluation method suggested in Appendix A have to be very cautiously interpreted. Or in other words: In case the computed functions $N_{ss}(E)$ and $\sigma(E)$ possess a complex structure, two or more types of interface states must be assumed. The numerical result is then doubtful, unless other tests reveal the reverse.

V. Measurements on p-type MOS structures

The measurement of interface states on p-type MOS diodes has presented particular features all the time:

(i) Conductance measurement: The properties of p-type MOS diodes have not been possible to be measured as closely to the majority carrier band edge as it was possible on n-type MOS samples. There are two reasons for this difficulty /2/:
First, the capture cross sections for holes are smaller than the capture cross sections for electrons. Therefore, and because the relaxation

frequency of the interface state under investigation must be chosen according to the frequency range prescribed by the conductance measuring equipment, the measurements have to be performed at bias regions where the capacitance dispersion is small. In consequence, the p-type samples can only be analysed with reduced accuracy compared with n-type samples.
Second, a limit of the conduction method is reached when the surface potential fluctuations become larger (cf. Fig. 17 and 18 in /2/). This occurs both for n-type and p-type samples at low temperatures, for p-type samples, however, to a larger extend. In case of large surface potential fluctuations data fitting becomes difficult because of an increasing error propagation.

(ii) DLTS measurements: The interface state density N_{ss} of p-type MOS diodes when measured with the CC-DLTS method, has shown a clear decay towards the valence band edge (Fig. 9 taken from Schulz /3/). This observation is in strong contrast to the results of quasistatic measurements.

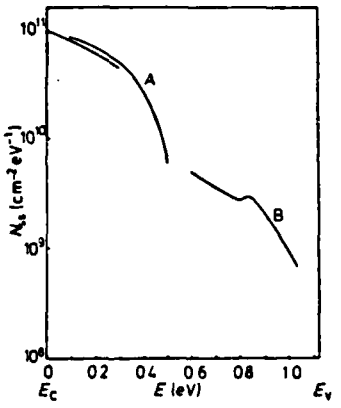

Densities of interface states as measured by CC-DLTS for MOS capacitors on n-type (curve A) and p-type (curve B) silicon. The decay observed for p-type samples seems to be a continuation of the variation observed in n-type material. The strong increase in the density of states shown in figure 3 is not visible.

Fig. 9 Densities of interface states as measured by the CC-DLTS method and evaluated by the former mathematical procedure (from M. Schulz /3/).

Considering the latter inconsistency with respect to the improved evaluation of the CC-DLTS method one must infer that the capture cross sections $\sigma(E)$ of p-type MOS structures are likely to increase towards the valence band. The correction factor with the term $d \ln \sigma / dE$ previously neglected in eq. (1) will then change the decay of N_{ss} into an increase if it is taken into account.

Moreover, capture cross sections increasing in such a manner will also explain the difficulties found in the conduction method with p-type samples:

As long as the capture cross sections slowly decrease with respect to energy towards the majority carrier band, they may be taken stepwise constant without severely affecting the results of the conductance method (Deuling et al. /4/). As can be shown, this does not hold in case the capture cross sections increase or strongly decrease. The relaxation broadening then appears to be intensified. It looks as if the surface potential fluctuations have increased. It is just this observation which is found in p-type samples.

Therefore the measurements on p-type MOS structures have been important not only to test the applicability of the CC-DLTS method but also to look for positive evidence for increasing capture cross sections.

At first we chose p-type samples with rather high interface state densities for the experiments. By this we wanted to anticipate troubles arising from signals too weak. We had to learn, however, that these samples showed a temperature hysteresis when measured with the CC-DLTS method, although the stability sufficed the requirements of the conductance and the quasistatic measurements. An example is given in Fig. 10. We did not investigate the cause of this instability.

We later got a p-type MOS diode of lower interface state density which was stable enough to be measured by the quasistatic, the conductance and the CC-DLTS method. It was an MOS diode, which was oxidized in a flow of oxygen and HCl at 1000 ^{o} C to 117 nm after the usual cleaning. Two annealing processes followed: one (10 min, N_2 , 1000 ^{o} C) directly after the oxidation, the other (30 min, N_2/H_2 , 450 ^{o} C) after the metalisation of the aluminum dots. We used epi-silicon (100). The upper layer (10 µm thick) had a doping density of 3.2×10^{15} cm^{3} . The oxide of the back side was removed. Aluminum was evaporated to form the back contact.

The quasistatic measurement and the complete conductance measurements were performed as described in /2/. A few conductance measurements were carried out according to a more economical procedure /5/. We only used this procedure in order to obtain several capture cross sections in addition without evaluating for the density of interface states and surface potential fluctuations.

The evaluation of the CC-DLTS measurements yielded results that looked quite wrong at first, in particular the capture cross sections differed considerably from the results of the conductance measurements. In order to make the search for the fault easier we calculated the correlation signals to be expected from the data of the conductance method. It turned out that there was hardly any principal fault to find in the CC-DLTS measurements. The poor results were chiefly caused by error propagation.

Therefore, in order to compare the methods on a reasonable basis, we modified the evaluation of the measured correlation signals by including the capture cross sections obtained by the conductance method. In particular we proceeded in the following way:

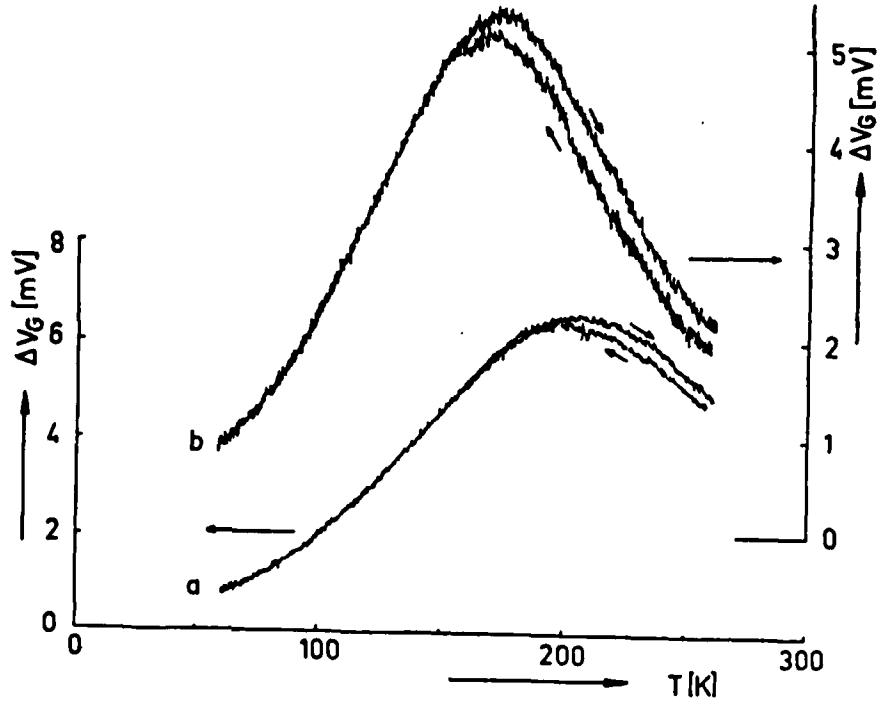

Fig. 10 Correlation signals of a p-type MOS diode with a high density of interface states.
This MOS diode (doping density 1.5×10^{16} cm^{-3}) was oxidized at 975 °C in a wet atmosphere to 100 nm. The interface state density as measured by the conductance method is about 10^{11} $V^{-1}cm^{-2}$. At low temperatures the correlation signals have been reproducible. Only at temperatures greater than 170 K the readings for increasing and decreasing temperatures, however, have been different. Each temperature run took 90 min.
We did not look for the cause of this instability, and we have not attempted to evaluate these curves, because the results of the conductance method yielded that data of the instable region were needed for the CC-DLTS evaluation. The sampling times were 2.5 ms/5 ms (curve a) and 25 ms/50 ms (curve b).

The two measured correlation signals were smoothed by averaging the noise components by visual judgement. These were the curves that gave the bad results. Next, a capture cross section σ and its derivative $D = d \ln \sigma / dE$ was then selected from the curve obtained by the conductance method (Fig. 11). According to eq. A.4 temperatures T_1 and T_2 were calculated for the two correlation signals (with the sampling times t_1 and t_2, resp.). For each of the two correlation signals there exist two equations of the kind like eq. (1). From these two equations $N_{ss}(E_o)$ can be eliminated:

$$(3) \qquad \frac{\Delta V_G\,(t_1\,,\,T_1)}{\Delta V_G\,(t_2\,,\,T_2)} = \frac{T_2}{T_1} * \frac{1 + kT_1 * D}{1 + kT_2 * D}$$

The terms on the left side of this equation are correlation signals obtained by CC-DLTS measurement only. On the right side there are only terms that are known from conductance measurement. They were either calculated from eq. A.4 or taken from Fig. 11.

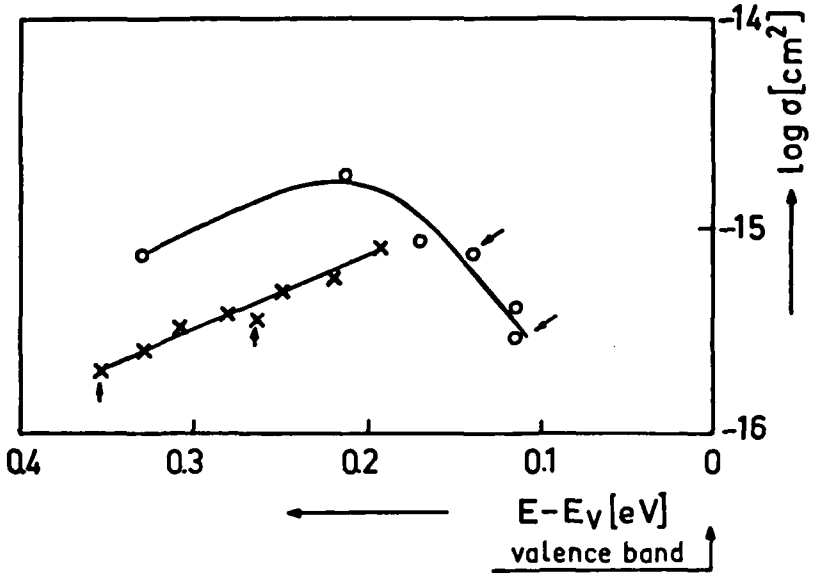

Fig. 11 Capture cross sections of a p-type MOS capacitor. The measurements were performed on two capacitors of the same wafer by the conductance method. Each of the measuring points comes from a different temperature, except the points with the arrows. They were measured at room temperature (crosses) and at 142 K (circles). The parallel shift of the two curves is caused for the most part by having computed the two curves with slightly different sets of basic constants (energy gap, its temperature coefficient, effective mass of holes, etc.). An error of 20 % in the doping density will affect the value of the capture cross sections by a factor 2, but all points will shift in the same way, virtually independent of temperature.
We gather from this figure, that the capture cross sections of p-type MOS samples first increase. Then they decrease towards the valence band edge as n-type samples do towards the conduction band edge.

By this we are able to check the consistency of the measured correlation signals at the temperatures (T_1, T_2) with the capture cross sections of the conductance method. We did so for several pairs (T_1, T_2). In case we did not find an agreement we increased the value of one correlation signal and reduced the value of the other one by the same percentage until eq. (3) was fulfilled. We found that these alterations of the correlation signals were by no means serious. Except for low temperatures there was only need to vary the correlation signals by 2 % at most. We regard this alteration to be within the expected errors.

In order to simplify the computer evaluation we did not directly use these modified correlation signals, but from them we constructed a polygonal trace in steps of 10 K (Fig. 12).

As the correlation signals were changed only to a small amount we may infer that the CC-DLTS evaluation of these correlation signals yields an interface state density N_{ss} independent of the results of the conductance method. The interface state density as obtained by the three methods are shown in Fig. 13.

As stated in the caption of Fig. 13 the question remains open whether the decrease of N_{ss} as measured by the DLTS method is only an artifact of the method or really exists. On the other hand the measurements show clearly, that in the energy ranges where the three methods overlap no contradiction between the results of the three methods can be discovered.

Further results were obtained by the conductance measurements: The capture cross sections (for holes) increase in midgap, but later the increase changes to a distinct decrease towards the valence band (Fig. 11). The increase of the capture cross sections, however, is too small to affect the results of the conduction measurements by giving the false impression of a broader relaxation range. The increase is also too small to alter the decrease of N_{ss} into an increase when evaluating the CC-DLTS measurements.

There is still an objection to the increase of the capture cross sections: Usually the doping density is assumed to be constant when the measurement data are evaluated. This assumption, however, does not hold in reality.

During the oxidation of the silicon wafer the dopant is redistributed in a zone near the interface. In p-type capacitors with boron as dopant the doping density is lowered at the interface. A rough estimate shows that taking the redistribution into consideration the increase of the capture cross sections will be smaller. We have not yet treated this problem quantitatively. An experimental test reveals that the effect is probably not great: In Fig. 11 two pairs of points are marked by arrows. Each pair was measured at the same temperature (whereas each of the other points were measured at different temperatures). Within each pair (of the same

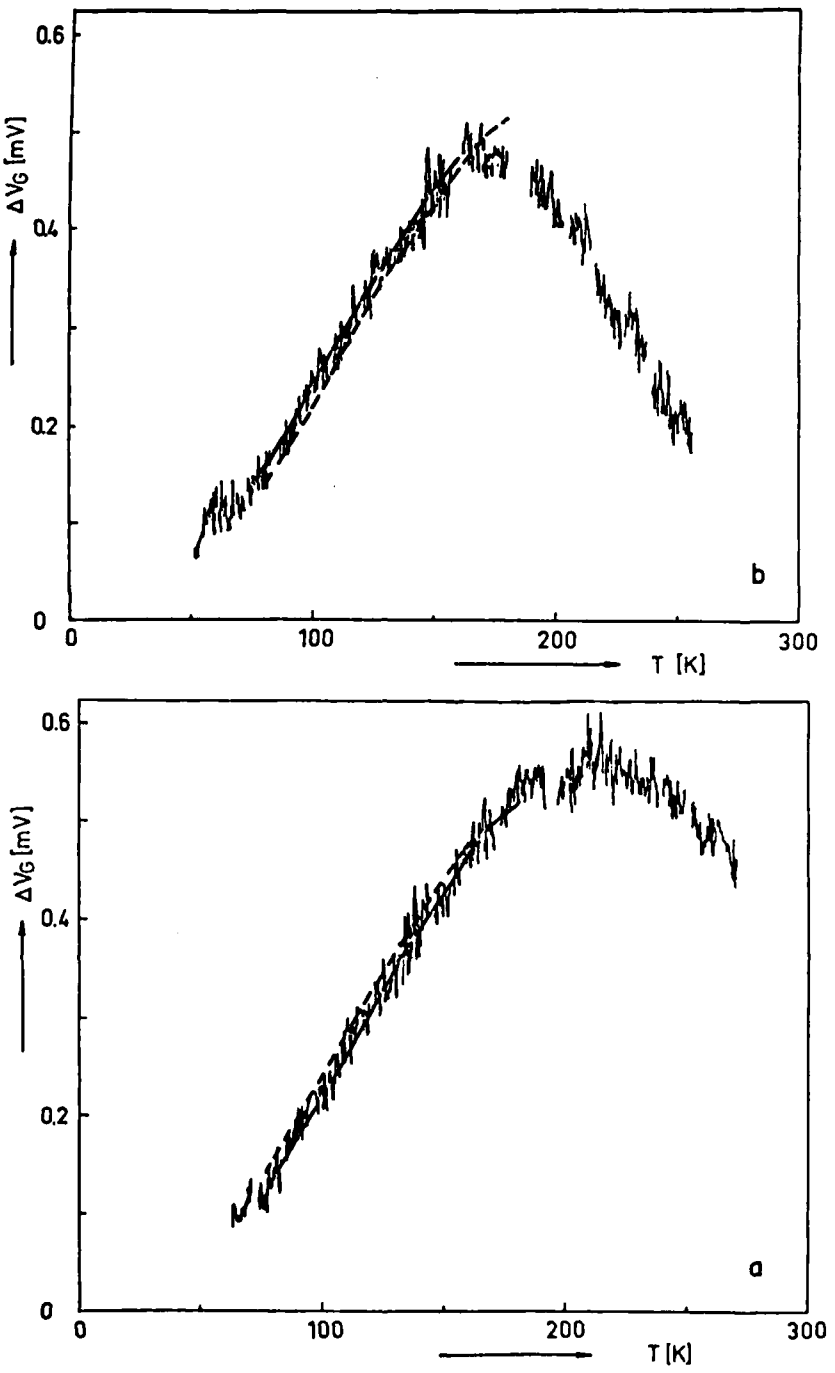

Fig. 12 Correlation signals of the p-type MOS capacitor. The sampling times were 2.5 ms/5 ms for curve a and 25 ms/50 ms for curve b. The capacitance was kept constant at $C/C_{ox} = 0.518$, which corresponds to a surface potential of $\psi_s^{ox} = 0.29$ V at 300 K. For the computer evaluation the measured curves were "averaged" in a manner which is fully described in the text. These values are represented by the solid polygonal traces. In order to make the differences between the two correlation signals more easily visible the corresponding curve with the other sampling times is inserted as a broken line.
The curves of the Fig. 13, 14, 15 were computed from these polygonal traces.

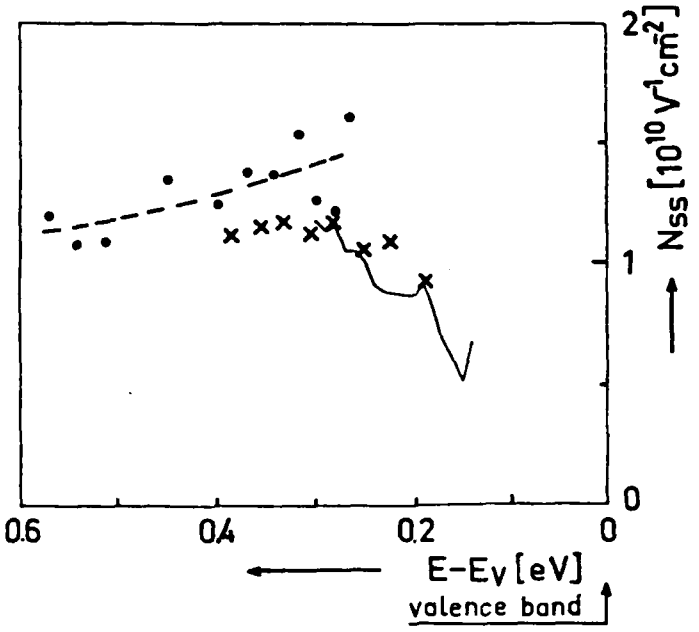

Fig. 13 Interface state density of a p-type MOS capacitor.
The interface state density was measured by three methods: the quasistatic method after Kuhn (full dots and broken curve), the conductance method (crosses) and the CC-DLTS method (solid curve).
The interface state density as measured by the CC-DLTS method and evaluated by the improved mathematical procedure still decreases towards the valence band edge (cf. Fig. 9). It is not possible, however, to verify or refute this decrease by the other measuring methods. The vestige of a decay, that can be seen in the crosses of the conductance method, is only supported by the cross at the very right. If this measuring point was absent, one would rather draw the conclusion that the density of interface states is constant.
The quasistatic measurement indicates a slight increase. Considering the scattering errors it is likely, however, that this indication is not real. By the way, the error that is common to all points of the quasistatic method amounts to about 35 %. The broken line can therefore be shifted up and down considerably.
The question about the decay of the interface states towards the valence band is still open. A positive result of this investigation is, that the three methods agree well in the region where they overlap.

temperature) the points distinguish themselves by having a space charge layer of different depth. The mean doping densities as seen by the space charge layers are therefore different as well. Although the mean doping densities are different, the capture cross sections fit very well to the genaral trend of the curves. Consequently we can conclude that the effect of redistribution is hardly of any importance.

At the begin of this paragraph two causes have been stated by which the conductance measurements are limited. One cause is found in the rather small capture cross sections. As explained above the bias has to be shifted into regions of the capacitance curve where the capacitance dispersion is small and the error propagation therefore is great.

In contrast to an expectation mentioned at the beginning, the surface potential fluctuation, which normally increases with decreasing temperature when measured in kT/q-units, did not put an end to the evaluation of the conductance measurements of this sample. Even at the lowest temperature (170 K) the surface potential fluctuation was only $\sigma_g = 1.65$.

Another cause, however, is found in a contribution of the back contact to the conductance of the total network. At low temperatures and at high frequencies it gets more and more difficult to separate this contribution from the losses of the interface states.

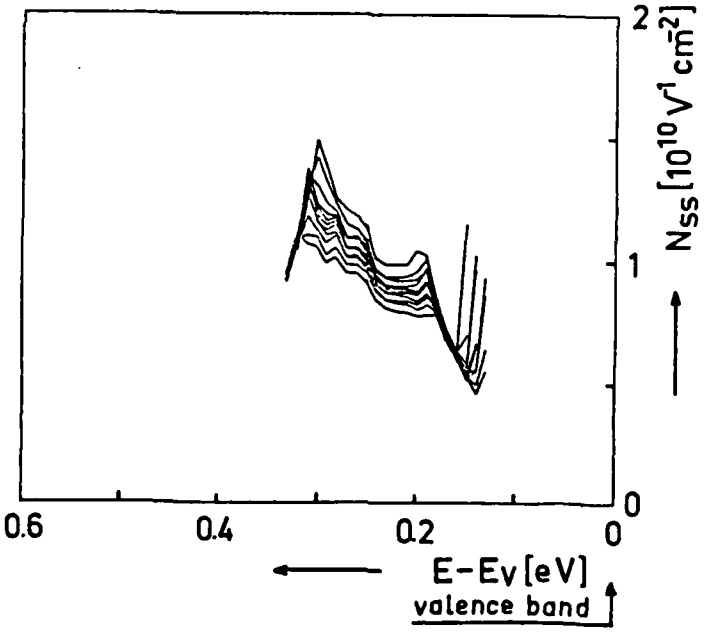

Fig. 14 Error analysis of the interface state density of the p-type MOS capacitor.
The error propagation was investigated in the same manner as it was done with the n-type sample (cf. Fig. 5).

An analysis of the error propagation (Fig. 14 and 15) was carried out in a similar way as it was done for the n-type sample (paragraph III). One has to note that the magnitude of the errors(1 % at most, 0.5 % on the average), from which this analysis started, are less than the actual errors of the measurement of the p-type sample. On the other hand, the wide spread of N_{ss} in Fig. 14 is chiefly caused by the great error of the slope of σ . In case the slope of the capture cross section is known (as it is in this paper from conductance measurements), the error of the density of interface states is almost only given by the error of the correlation signals.

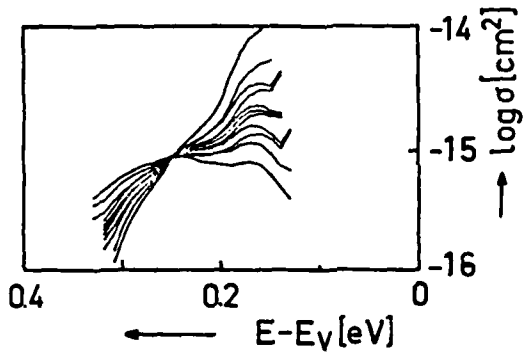

Fig. 15 Error analysis of the capture cross sections of the p-type MOS capacitor.
(cf. Fig. 14 and Fig. 6).

VI. Conclusions

We have shown by our study that the CC-DLTS method can be a valuable means to investigate the interface properties of MOS structures. At the time being, however, this method cannot yet replace the other usual methods, e.g. the quasistatic method and the conductance method.

In order to adjust the CC-DLTS equipment to the sample under investigation a high frequency capacitance measurement as a function of the bias has to precede the CC-DLTS measurement in future, too. In these circumstances nearly no additional effort is required to complement the hf-capacitance measurement by a slow ramp measurement and then evaluate the readings according to the quasistatic method after Kuhn. The profit of having full information by the quasistatic method will generally be more useful than the advantage of dispensing with an additional capacitance measurement.

The CC-DLTS technique can be very advantageous even in its simple arrangement, where only N_{ss} in dependence on T is measured (cf.

paragraph I). In this case the CC-DLTS equipment does not need particularly sophisticated instrumentation, especially the same capacitance bridge as for the c-v-measurement and a simple cryostat may be used. The two methods, i.e. the quasistatic and the CC-DLTS method, complement one another very well because the CC-DLTS technique is more sensitive in respect to N_{ss} than the quasistatic method (whose limit is reached at about 10^{10} V^{-1} cm^{-2}). This technique will be well suitable for routine measurements, for example for weekly random tests in production lines.

The situation is different, if we compare the CC-DLTS technique with the conductance technique. As shown in Appendix A it was just possible to evaluate a sample with an interface state density of $N_{ss} = 10^{11}$ $V^{-1}cm^{-2}$. We saw in paragraph V that a sample with $N_{ss} = 10^{10}$ $V^{-1}cm^{-2}$ could only be evaluated after some results of the conductance method had been consulted.

In order to make the CC-DLTS method a serious competitor to the conductance method, the experimental setup has to be considerably improved in data acquisition and processing. As one can conclude from the error analysis shown in Fig. 5/6 and Fig. 14/15, it is mandatory that the errors of the correlation signals are reduced to distinctly less than 1 %. Moreover, it is advisable to use more than two correlation signals. Proceeding in such a way does not only reduce the errors, but one can also accomplish an Arrhenius-plot (τ -T plot). By it the validity of some presuppositions (independence of the capture cross sections of temperature or electric field, etc.) can be checked. The mathematical procedure suggested in Appendix A can easily be generalized to handle more than two, say n, correlation signals. The equations like eq. A.9 then form an overdetermined system of n equations, which can be solved by a least square method.

Such an extensive measuring task can only be accomplished with an on-line computer operation. Then the correlation signals should no longer be developed electronically but in the computer itself. The data stored have to be the voltage transients at several points of time, for instance 1 ms, 2 ms, 4 ms, ... 128 ms. By this, 7 correlation signals can be generated. It will be sufficient to measure these voltage transients in 3 - 4 K steps from about 50 K to 300 K. We estimate that each transient has to be averaged by more than 100, maybe even 1000 runs. As can be seen from the following the increase of time needed for an improved data acquisition is the limiting factor to a full CC-DLTS evaluation. The measuring time will be:

Number of transients:	$\frac{300 - 50}{3} = 84$
Duration of each transient:	0.15 s
Duration for stabilizing the temperature after each step:	60 s
Total time of the measurement:	$84 \times (200...1000) \times 0.15 + 84 \times 60$ $= (7.5...18) \times 10^3$ s = (2...5) hours

We expect that a full evaluation is only successful with samples of more than 10^{10} interface states/V · cm^2 .

There are still two points concerning the mathematical procedure, which must not be overlooked:

First, the correlation signals recalculated with a solution $N_{ss}(E)$, σ (E) differ from the starting correlation signals by 0.5 % to 1 %. The other way round, improving the accuracy of the measured correlation signals to better than approximately 1 % will be of no avail, because the inherent error of the mathematical approximation then prevails.

Second, as pointed out in Appendix A the starting equations of the CC-DLTS problem consist of a system of integral equations. So far nothing is known about the solutions and especially nothing about their manifoldness. It is likely that there are still more solutions than those given in Appendix A.

The suggested solutions may probably be distinguished from the other hypothetical ones by being "most smooth": Within an energy interval ΔE determined by the weighting function (Fig. A.2) the functions $N_{ss}(E)$ and σ (E) are represented by only a single value each and the higher derivatives of N_{ss} and $\ln \sigma$ are stepwise constant or vanishing.

One has to expect that the solutions of the hypothetical type are represented by more than one value in each interval, so that the higher derivatives do not vanish and thus the two functions N_{ss} and σ vary strongly within short distances.

These solutions can either oscillate across the approximations given in Appendix A, or they can diverge from these old solutions. According to our measurements, the "smooth" functions are seemingly the solutions adequate to the CC-DLTS problem. Then the question arises why nature excludes these hypothetical solutions and prefers the "smooth" curves. This answer has to be the task of a future investigation.

Literature

/1/ E. Klausmann
The Evaluation of Transient Capacitance Measurements on MOS Interfaces
Insulating Films on Semiconductors 1979
(Inst. Phys. Conf. Ser. No. 50) p 97

/2/ A. Goetzberger, E. Klausmann, M.J. Schulz
Interface States on Semiconductor/Insulator Surfaces
CRC Crit. Rev. Solid Sci. 6, 1 (1976)

/3/ M. Schulz
MOS Interface States
Insulating Films on Semiconductors 1979
(Inst. Phys. Conf. Ser. No. 50) p 93

/4/ H. Deuling, E. Klausmann, A. Goetzberger
Interface States in Si-SiO_2 Interfaces
Solid State Electr. 15, 559 (1972)

/5/ M. Warashina, A. Ushirokawa
Conductance(G)-Bias(V) Method for Interface States in MOS Structure
Jap. J. Appl. Phys. 14, 1739 (1975)

Appendix A

(Insulating Films on Semiconductors, 1979
Edited by G.G. Roberts and M.J. Morant)

Inst. Phys. Conf. Ser. No. 50: Chapter 2 97

The evaluation of transient capacitance measurements on MOS interfaces

E Klausmann
Fraunhofer-Institut für Angewandte Festkörperphysik, Eckerstrasse 4, D-7800 Freiburg, West Germany

Abstract. A new procedure is developed for evaluating the density of interface states and capture cross sections of MOS interfaces by means of the CC–DLTS method. The procedure used hitherto was based on rather restrictive assumptions. The solution cannot be determined unambiguously with only two sets (correlation signals) of measured data. Additional data are required, either from CC–DLTS measurements or the conductance method, to establish the uniqueness of the solution. An experimental comparison of the CC–DLTS and conductance methods is presented.

1. Introduction

The conduction method is generally considered to be the standard procedure for analysis of the properties of the interface states of MOS structures (Nicollian and Goetzberger 1967, Deuling *et al* 1972, Goetzberger *et al* 1976). This method has been used to obtain the most reliable results on the energy distribution of the densities of interface states and capture cross sections over a wide range of energies. The biggest drawback is, however, the great amount of time needed for the measurements and the necessity for the measuring equipment to be permanently attended when in operation. Some progress towards obtaining conductance measurements more rapidly has recently been achieved by a lock-in amplifier technique (Boudry 1978).

A strong competitor to the conduction method has recently emerged in the CC–DLTS technique (constant-capacitance deep-level-transient spectroscopy; Johnson *et al* 1978, Schulz and Klausmann 1979). The most striking advantages are the short measuring time (about ten times faster than the conventional conductance method) and the semi-automatic operation that only needs occasional supervision.

The competitive aspect should not, however, be stressed too much. As pointed out in the papers cited, the two methods also complement each other. For instance, results obtained by the CC–DLTS method are hardly affected by fluctuations in the surface potential and measurements made at low temperatures are more easily interpreted. Information about the statistical distribution of the oxide charges is only provided in full detail by the conductance method. However, the validity of these statements is not as strict as was claimed previously, a result that is a by-product of this paper.

In an experimental comparison of the two methods, some differences in the results were observed. A closer inspection of the procedure used to evaluate the CC–DLTS method showed that some assumptions did not really meet the actual conditions. The

0305-2346/80/0050-0097$02.00

most severe restriction exists in the presupposition that the capture cross sections should be stepwise constant, i.e. independent of energy over small intervals. If this presupposition is abandoned, it will be found that the mathematical treatment no longer results in a unique solution: the density of interface states and capture cross sections are then represented by a family of curves. Only after additional measurements can the proper result be selected.

2. Experimental details

To verify the applicability of the suggested method, a practical example with an n-type silicon MOS capacitor is given here. The capacitor is on a (111)-oriented wafer with an oxide thickness of about 100 nm and a doping density of about $5 \times 10^{15}\,cm^{-3}$. A great many conductance measurements have been performed previously with capacitors of the same wafer (Deuling *et al* 1972, Ziegler and Klausmann 1975). The conductance data given here have been taken from these papers. Further details about the wafer and its preparation can be found there. Checks were carried out to assure that the wafer had not changed.

In the papers mentioned above, the conductance and CC–DLTS method and the instrumentation involved has been described comprehensively; therefore only the basic ideas behind the CC–DLTS technique are outlined here.

3. The CC–DLTS method

The CC–DLTS method can be used to analyse the density of interface states, the capture cross sections and the energy levels of these states in MOS capacitors. The method makes use of the time and temperature dependence of the electron (or hole) emission from the interface states into the majority carrier band. Firstly the states are occupied by electrons during a voltage pulse (20 μs) into the accumulation regime. Then with the bias in depletion, the excess charges are thermally emitted. In the CC–DLTS method the bias V_G is controlled by a feedback circuit in such a way as to keep the high-frequency MOS capacitance C constant. Consequently the band bending also stays virtually constant during emission and evaluation is made considerably easier.

The time-dependent bias $V_G(t)$ is then sampled at two different times t_l and $t_l^* (= 2t_l)$ and the difference $\Delta V_G(t_l) = V_G(t_l) - V_G(t_l^*)$ (correlation signal) is obtained. By varying the temperature, the emission rate is changed and the correlation signal shows a maximum at an optimum temperature for a particular interface state. For states of different energy and different capture cross section, the maximum occurs at different temperatures. The correlation signal $\Delta V_G(t_l, T)$ is recorded as a function of the temperature T with the sampling times $(t_l, 2t_l)$ as parameters.

In the papers cited above it has been shown that the correlation signal is related to the pertinent physical quantities by

$$\Delta V_G(t_l, T) = \frac{A}{C_{ox}} \int_{E_s}^{0} N_{ss}(E) \left[\exp\left(-\frac{t_l}{\tau(E)}\right) - \exp\left(-\frac{2t_l}{\tau(E)}\right) \right] dE \qquad (1)$$

and

$$\tau^{-1} = \sigma(E)\, v_{th} N_C \exp(E/kT). \qquad (2)$$

Here A is the area of the MOS capacitor, C_{ox} is the oxide capacitance, E is the energy level of the interface state within the band gap (referred to the majority carrier band edge), E_s is the energy of the deepest state that can just be charged and discharged by the bias V_G (see figure 1) and $N_{ss}(E)$ is the density of interface states. $\sigma(E)$ is the capture cross section, $\tau(E)$ is the response time of an interface state, t_l is the sampling time, k is the Boltzmann constant, T is the temperature, $v_{th} = 10^7 (T/300)^{1/2}\,cm\,s^{-1}$ is the thermal velocity of electrons and $N_C = (2{\cdot}8 \times 10^{19})(T/300)^{3/2}\,cm^{-3}$ is the effective density of states in the conduction band. The numerical values given here refer to electrons as majority carriers in silicon.

The energy E_s can be obtained by high-frequency capacitance or slow ramp measurements (Kuhn 1970). Equation (1) with $i = 1, 2, \ldots$ (together with equation (2)) composes a system of integral equations with the unknown functions $N_{ss}(E)$ and $\sigma(E)$. All other quantities are known or, at least in principle, are amenable to measurement. In a strict mathematical sense, however, nothing is known about a solution, its existence and uniqueness and how many correlation functions with different t_l must be given for such a solution.

In the following the problem will be described approximately by differential equations. Two correlation signals with different t_l will suffice to achieve solutions for practical purposes. These solutions, when put into equation (1), reproduce the measured correlation signals to an accuracy of 1% or better. The measurement of a third correlation signal will be necessary to determine the final solution unambiguously unless additional data obtained by the conductance method are used.

3.1. Preparatory mathematical transformations

It is presupposed that the interface states can only be described by a single pair of functions $N_{ss}(E)$ and $\sigma(E)$. These functions must be continuous and differentiable if required. The following developments do not hold if two (or more) types of interface states with different capture cross sections $\sigma_1(E)$ and $\sigma_2(E)$ are present, as may be expected in contaminated MOS structures.

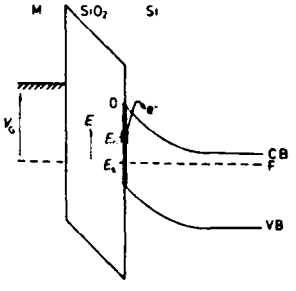

Figure 1. Thermal emission in the energy band model. Electrons are released from occupied interface states above the Fermi level, but only electrons from a small energy interval ΔE in the neighbourhood of the mean energy E_s contribute to the correlation signal. At sufficiently low temperatures this interval is far above the energy E_s and the correlation signal is therefore independent of this parameter. At higher temperatures and for a sampling time that is not too short, E_s approaches E_s and at its lower end the interval ΔE is limited by E_s. As a consequence, the correlation signal drops steeply. V_G is the bias voltage, the Fermi level is labelled F and the edges of the conductance and valence bands are marked CB and VB respectively. The energy E_s is given by that point in the band gap at which the Fermi level pierces the interface.

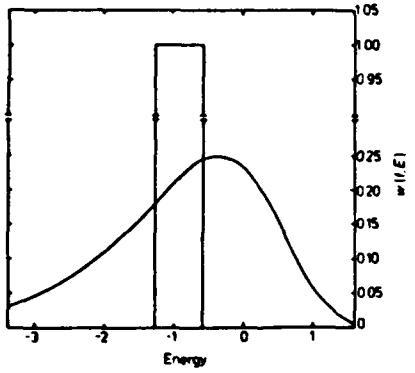

Figure 2. The weighting function $w(t, E)$. It is assumed that $\sigma(E)$ is constant and does not depend on energy. The abscissa represents an energy axis in units of kT/q (it may include an additive constant). If $N_{ss}(E)$ is a smooth function, integral (1) can be approximated by an explicit function (equation 3), which is equivalent to replacing the weighting function by the rectangular function. Its width is given by equation (6), $\Delta E = kT \ln 2$. These formulae can still be retained in the general case, when $\sigma(E)$ actually depends on energy, by adding a correction factor which contains the logarithmic derivative of $\sigma(E)$ (equations 9 and 10).

Let us initially assume that the capture cross sections are constant and independent of energy and that the temperature is sufficiently low. The integral (1) is then independent of E_s, which can be replaced by $-\infty$ (figure 1). The weighting function $w(t, E)$ in the integrand (the expression in square brackets in equation 1) is sharply peaked (figure 2). Its halfwidth amounts to approximately $\pm 1{\cdot}2\ kT$ units. On the condition that the density of interface states $N_{ss}(E)$ does not change very much within the range of halfwidths considered, the integral can be calculated exactly:

$$\Delta V_G(t_1, T) = (kT/q)(A/C_{ox})qN_{ss}(E_0)\ln 2. \tag{3}$$

In this equation $N_{ss}(E_0)$ represents an averaged value of the density of interface states in the vicinity of the maximum of the weighting function.

In calculations used previously in the literature, the abscissa of the maximum of the weighting function has been determined to be E_0. It is better, however, to take for E_0 the abscissa of the centre of gravity of the area under the weighting function curve. Then equation (3) is still exactly valid not only if N_{ss} is constant but also if $N_{ss}(E)$ is a linear function of E:

$$E_0 = -kT \ln(\sigma(E_0)v_{th}(T)N_C(T)2{\cdot}52t_1). \tag{4}$$

This assignment can be interpreted more clearly. Transformation of equation (4) and comparison with equation (2) leads to

$$\tau = 2{\cdot}52t_1. \tag{5}$$

This means that by the choice of the sampling times $(t_1, 2t_1)$ just those interface states are selected which possess the response time τ.

Moreover, it can be deduced from equation (3) that the energy interval in which the interface states that make the greatest contribution to the correlation signal are located is given by

$$\Delta E = kT \ln 2. \tag{6}$$

Hence in the regime for which these approximations are valid, the weighting function of the integral (1) is replaced by a rectangular function (also shown in figure 2).

The assumption that the capture cross sections should be constant can easily be dropped. Let us develop $\sigma(E)$ in the vicinity of E_0:

$$\sigma(E) = \sigma(E_0)\ \exp[\gamma \times (E - E_0)] \tag{7}$$

where γ is the logarithmic derivative of σ at $E = E_0$:

$$\gamma = \mathrm{d} \ln \sigma(E)/\mathrm{d}E. \tag{8}$$

From equation (2) the expression

$$\tau^{-1} = \sigma(E_0)\, v_{th} N_C \exp\left[\left(\frac{1 + \gamma kT}{kT}\right)(E - E_0) + \left(\frac{E_0}{kT}\right)\right]$$

can be obtained.

It can be shown that only the factor by which E is multiplied affects the value of the approximation to integral (1); the additive constant is of no importance. Therefore equations (3) and (6) are still valid if $kT/(1 + \gamma kT)$ is substituted for kT:

$$\Delta V_G(t_1, T) = (A/C_{ox})N_{ss}(E_0)\Delta E \tag{9}$$

and

$$\Delta E = \frac{kT \ln 2}{1 + kT(\mathrm{d} \ln \sigma(E)/\mathrm{d}E)|_{E=E_0}}. \tag{10}$$

Equation (4) may be retained. In this more generalised representation, E_0 can still be interpreted as the centre of gravity of the weighting function. It must be remembered, however, that these equations are only valid if the integral (1) is independent of E_s, i.e. the interval $E_0 \pm \frac{1}{2}\Delta E$ must be far enough away from E_s. To meet this condition, ΔV_G must be measured at temperatures that are not too high and at sampling times that are not too long. The system of integral equations can now be replaced by a system of differential equations (equation 9 with $i = 1, 2, \ldots$ and equation 4) that can be solved numerically.

3.2. *Method of solving the differential equations*

This method originates from a procedure suggested by K Nickel (1979 private communication). To begin with, any value $\sigma(E_0) = \sigma_0$ at any energy E_0 is chosen arbitrarily; and the following three steps are then carried out.

Step 1. Temperatures T_i to be associated with the sampling times t_i are calculated in such a way that equation (4) is fulfilled

Step 2. These T_i are put into the system of equation (9). These equations must be considered to be conditional for the two unknown quantities

$$N_{ss}(E_0) \text{ and } \gamma = \mathrm{d} \ln \sigma(E)/\mathrm{d}E|_{E=E_0}.$$

Two equations and hence two correlation signals are sufficient to calculate the two unknowns.

Step 3. With equations (7) and (8) and $E = E_0 + \delta E$, another capture cross section $\sigma(E)$ can be calculated. The increment δE may be positive or negative but must be sufficiently small. The quantity E will now be denoted E_0.

Steps 1–3 may then be repeated and in this way functions $N_{ss}(E, \sigma_0)$ and $\sigma(E, \sigma_0)$ can be established. The arbitrarily chosen σ_0 serves as an integration constant. The procedure stops by itself when the temperatures T_i are too high or too low and the corresponding correlation signals fall outside the measured range. It must be stopped in cases where the basic equation (9) is no longer valid. This happens when the temperature T_i approaches the region in which the correlation signal is reduced as a consequence of E_s limiting the emission.

Figures 3, 4 and 5 show the results of a practical example. The necessary explanations are found in the figure captions. Most striking is the large spread of the curves that

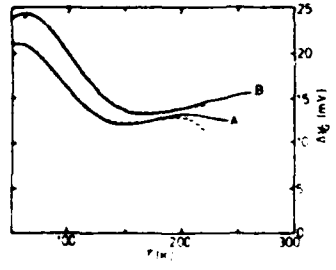

Figure 3. Correlation signals. The full curves are the measured correlation signals for $t_1 = 2.5$ ms and $t_2 = 25$ ms. The capacitance, which was kept constant during the emission phase, was $C/C_{ox} = 0.537$; this is equivalent to E_s in the midgap. The broken curves were obtained from a check calculation by putting the values of the dotted curves of figures 4 and 5 into the exact equation (1). On average, the calculated and measured values agree to within 0.5% for curve A and 0.8% for curve B. In the method used hitherto, the errors amounted to 100%.

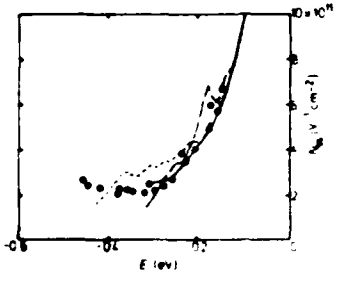

Figure 4. Density of interface states. For the sake of clarity, only three curves out of the family of density of interface state curves are drawn. These correspond to the broken curves in figure 5. The other interface state density curves lie quite close to those displayed in this figure. The points were obtained from conductance method measurements.

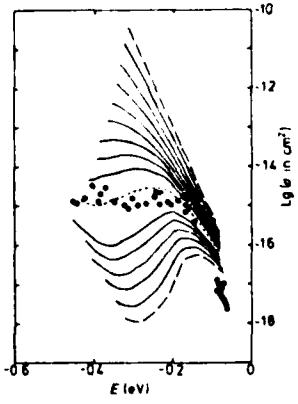

Figure 5. Capture cross sections. The family of curves is limited arbitrarily by the broken curves; the total spread is wider. The dotted curve is the best fit according to the conductance measurements (see captions to figures 3 and 4).

represent the capture cross sections $\sigma(E)$, whereas the corresponding curves for the density of interface states $N_{ss}(E)$ lie comparatively close together. It will be shown below how we may choose the proper functions $N_{ss}(E)$ and $\sigma(E)$ from these families of curves.

3.3. Determination of the integration constant

There are two possible methods:

(i) As has already been shown in figure 5, the capture cross sections can be fitted to values obtained by the conduction method. If in order to expedite the measurements only one or two capture cross sections have been measured by the conductance method, these fitting points should be selected from a suitable energy range, otherwise the errors propagate too much. As can be seen from figure 5 it seems advisable to choose them in the middle of the band gap rather than near the band edge.

(ii) The correlation signal is greatly affected by E_s when E_0 approaches E_s:

$$|E_s| \leq |E_0|. \tag{11}$$

The signal then decreases with increasing temperature (see figure 1).

We can use these facts to formulate a method for determination of the integration constant. To this end, we need only measure a third correlation signal with a reduced value of E_s (adjusted to a higher capacitance in the emission phase). The required value of E_s is obtained by HF capacitance or slow ramp measurements. Correlation signals can now be determined according to equation (1) with the solutions $N_{ss}(E, \sigma_0)$, $\sigma(E, \sigma_0)$ for different values of σ. All the quantities required for the computation are known. When evaluating equation (1), attention must be paid to the fact that E_s is temperature-dependent when the capacitance is kept constant. The energy E_s is the sum of the band bending and the Fermi energy

$$E_s = q\psi_s + kT \ln(N_D/N_C(T)) \tag{12}$$

where N_D is the concentration of dopant. The band bending ψ_s is also dependent on temperature to a small extent, but in the following this dependence will be neglected.

The correlation signals calculated for different values of σ_0 can be distinguished from each other by the steep slope that occurs at different temperatures for each signal. The correct solution can then be found by comparison of the different calculated values with the measured signal.

In figure 6, the two methods for determining the integration constant are cross checked. The full curve represents a correlation signal for the same capacitor as was used for figure 3. The sampling time was chosen as $t_1 = 2{\cdot}5$ ms and the normalised capacitance $C/C_{ox} = 0{\cdot}625$, which is equivalent to $E_s = -0{\cdot}389$ eV at $T = 300$ K. Other correlation signals were computed with different C/C_{ox} (dotted curves); no agreement was apparent and in particular, the measured curve was not nearly as steep as the calculated results.

This discrepancy is caused by not taking fluctuations in the surface potential into consideration. Surface potential fluctuations are a consequence of the statistical distribution of the oxide charges and the charged interface states of the MOS structure (statistical model of Nicollian and Goetzberger 1967). Measurements made by the conductance method verified that a good approximation to the behaviour of these fluctuations is given by a Gaussian distribution.

The influence of fluctuations in the surface potential can be taken into account in the exact equation (1). Good approximate results can also be achieved within the scope of the approximations from which equations (9) and (10) were obtained. Because only electrons from interface states above E_s participate in the emission, the energy interval ΔE given by equation (10) will be reduced if E_0 approaches or even surpasses E_s.

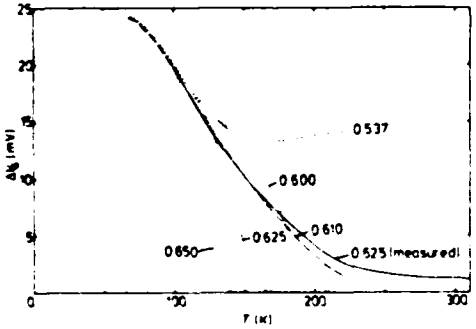

Figure 6. Fluctuations in the surface potential and correlation signals. Correlation signals with a sampling time $t_1 = 2{\cdot}5$ ms are presented. The full curve was measured for the same sample as was used for figure 3, all other curves are calculated. The initial data for the calculations were taken from the dotted curves of figures 4 and 5. The values shown for each curve give the normalised capacitances C/C_{ox} which were kept constant during the emission phase. For the dotted curves the steep slope is seen because the emission is limited by E_s. However, a discrepancy exists between the measurements and the calculations. It can be amended by taking surface potential fluctuations into consideration (broken curve) and in this way rather good agreement is obtained. A small but negligible difference remains in the normalised capacitance values.

Equation (10) must therefore be modified.

$$\Delta E = \int_{E_s}^{0} w(t, E)\,\mathrm{d}E = \frac{kT}{1 + kT(\mathrm{d}\ln\sigma/\mathrm{d}E)|_{E=E_s}}\, W\left(\frac{E_0 - E_s}{kT}\right). \tag{13}$$

It is almost evident and can easily be shown that this integral W is a function of $(E_0 - E_s)/kT$ only. The function W can be tabulated by numerical integration. From this the generalisation of equation (9) is obtained:

$$\Delta V_G(t_1, T) = \frac{A}{C_{ox}} N_{ss}(E_0)\, \frac{kT}{1 + kT(\mathrm{d}\ln\sigma/\mathrm{d}E)|_{E=E_s}} \times \int_{-\infty}^{+\infty} \frac{\exp\{-[q(\psi_s - \bar{\psi}_s)/kT]^2/2\sigma_s^2\}}{\sigma_s(2\pi)^{1/2}}\, W\left(\frac{E_0 - E_s}{kT}\right) \frac{q}{kT}\,\mathrm{d}\psi_s \tag{14}$$

where $\bar{\psi}_s$ is the mean surface potential related to E_s and σ_s is the variance by which the surface potential fluctuations are characterised.

Equation (4) is required when computing E_0 in equation (14). Here the approximation is slightly improved if the factor 2·52 in equation (4) is replaced by 2·06. The factor 2·52 only applies if the weighting function is integrated from $-\infty$ to $+\infty$. Then those values of $N_{ss}(E)$ that lie to the right- and left-hand sides of the centre of gravity of the weighting function and which deviate from $N_{ss}(E_0)$ cancel each other. This property is lost here because the integration starts at a finite lower limit.

When integrating equation (14), attention must be paid to the fact that the quantity E_s itself in the argument of W depends on the integration variable ψ_s (equation 12). The broken curve in figure 6 was computed. According to equation (14) the curve was fitted to the measured values by choosing the capacitance parameter to be $C/C_{ox} = 0{\cdot}61$, which is equivalent to $E_s = -0{\cdot}409$ eV at 300 K. For the variance σ_s a value of 1·8 was taken from conductance measurements and the well-tried approximation for its temperature dependence

$$\sigma_s \propto 1/T$$

was used (Deuling *et al* 1972).

The measured and the calculated curves agree well. In particular, the slope of the correlation signal can be seen to extend over a large range of temperatures when fluctuations in the surface potential are taken into account. The difference between the measured parameter E_s and the value of E_s used for fitting

$$\Delta E_s = 20\,\mathrm{meV}$$

is within experimental error.

4. Summary and conclusions

An improved approximation procedure for evaluating CC–DLTS data has been developed. The new method is more self-consistent than that used hitherto. The restriction that requires the capture cross sections to be independent of energy over small intervals is

abandoned, but as a consequence, the solutions for the density of interface states and the capture cross sections are no longer unique. To find the proper solutions, additional measurements, obtained by either the conductance method or by the CC–DLTS technique, must be performed. For the latter method, surface potential fluctuations are of considerable importance.

It is still difficult to give a general estimate of the errors involved in the CC–DLTS method. Densities of interface states can definitely be measured to less than $10^{10} V^{-1} cm^{-2}$, and in the experimental example given here, errors in calculating the capture cross sections amount to about an order of magnitude. An experimental comparison with the conductance method is given; agreement between the two methods is fair.

Acknowledgments

The author is indebted to Professor K Nickel for his valuable advice and to Dr K Eisele for numerous helpful comments. The technical assistance of Mrs A Helde is greatly appreciated. The work was supported by the US Army Research Office.

References

Boudry M R 1978 *J. Phys. E: Sci. Instrum.* **11** 237–47
Deuling H, Klausmann E and Goetzberger A 1972 *Solid St. Electron.* **15** 559–71
Goetzberger A, Klausmann E and Schulz M J 1976 *CRC Crit. Rev. Solid St. Sci.* **6** 1–43
Johnson N M, Bartelink D J and Schulz M 1978 *The Physics of SiO_2 and its Interfaces. Proc. Int. Topical Conf., Yorktown Heights* ed S T Pantelides (New York: Pergamon) pp421–7
Kuhn M 1970 *Solid St. Electron.* **13** 873–85
Nicollian E H and Goetzberger A 1967 *Bell Syst. Tech. J.* **46** 1055–133
Schulz M and Klausmann E 1979 *Appl. Phys.* **18** 169–75
Ziegler K and Klausmann E 1975 *Appl. Phys. Lett.* **26** 400–2

Appl. Phys. 18, 169--175 (1979)

Applied Physics

Transient Capacitance Measurements of Interface States on the Intentionally Contaminated Si–SiO_2 Interface

M. Schulz

Institut für Angewandte Physik, Universität D-8520 Erlangen, Fed. Rep. Germany

E. Klausmann

Institut für Angewandte Festkörperphysik, Fraunhofer-Gesellschaft, D-7800 Freiburg, Fed. Rep. Germany

Received 21 August 1978 Accepted 15 September 1978

Abstract. The constant capacitance transient capacitance technique (CC-DLTS) was applied to analyse the effect of impurities on MOS interface states. The elements Cs, Pb, Xe were ion implanted prior to oxidation. Sodium was implanted directly into SiO_2 and drifted to the interface. The alkali ions cause a steep increase in the density of interface states near the conduction band edge. The other elements studied show little effect on the interface properties. The capture cross-section for electrons decreases strongly near the conduction band.

PACS: 73.40

We have studied the effect of impurities on density and properties of MOS interface states. The influence of impurities in semiconductor insulator interfaces is not well understood, but it is expected that impurities have a strong effect since in recent years the density of states in MOS interfaces could be markedly reduced by improvement of cleanliness standards.

Ion implantation was used to introduce the impurity into the MOS interface for the study using the same technique, as previously published [1]. Ion implantation makes it possible to select special types of elements with high purity and to incorporate these elements directly into the interface in a controlled manner by choosing the appropriate energy. In order to avoid radiation damage in the interface we implant the impurity under consideration before oxidation into the bare silicon surface with a well controlled dose of the order 10^{12}–10^{14} cm^{-2}. The silicon wafer is then oxidised thermally with standard technology to obtain approximately 1000 Å thin SiO_2 layers. It is known that during formation of the oxide from the implanted Si-layer, the impurity redistributes itself to establish an equilibrium with the interface. As indicated in the schematic drawing of Fig. 1, most impurities are gettered in the interface region. A concentration profile with peaks in the interface and at the surface is generally observed by secondary ion mass spectroscopy SIMS [1, 2].

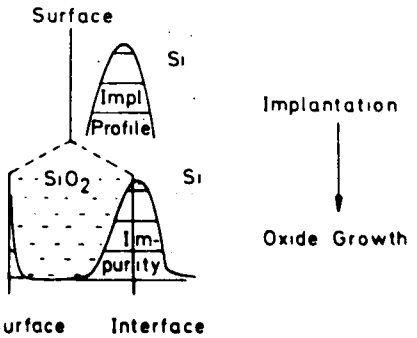

Fig. 1. Schematic drawing of the procedure to introduce an implanted impurity into the MOS interface

0340-3793/79/0018/0169/$01.40

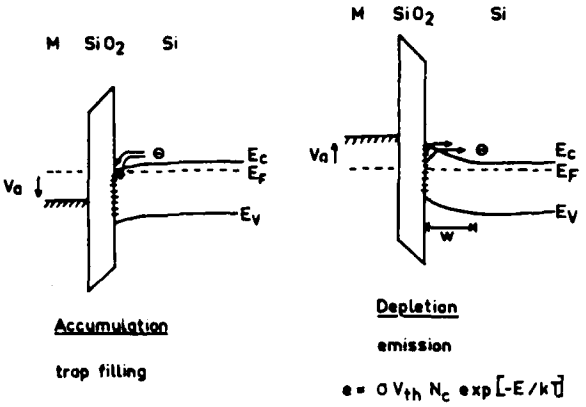

Fig. 2. Schematic drawing to illustrate the measurement principle of DLTS applied to an MOS structure

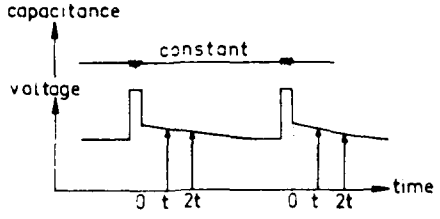

Fig. 3. Schematic drawing to explain the correlation procedure in the "Constant Capacitance Transient Spectroscopy" CC-DLTS

The new feature of the present paper is the application of the transient capacitance measurement technique DLTS to analyse the dynamic properties of MOS interface states in presence of impurities. The DLTS technique has been mainly used to measure bulk defects [3-5]. It has also been successfully applied to study MOS interface states in the case of state-of-the-art clean MOS interfaces [6–8]. The technique features high sensitivity and complements the conventional techniques, e.g. the quasistatic and conductance technique for measuring interface state properties, in that it is not affected by surface potential fluctuations which arise from the random spatial distribution of fixed positive charge in the oxide. The technique is therefore especially advantageous for measuring interface states at energies close to the band edge.

Details on the measurement technique and the evaluation analysis are given elsewhere [9]. Here we only explain the main details of the measurement procedure and evaluation. New results are shown for the interface state density distribution in presence of the alkali elements Cs and Na in the interface region. These elements are known to have a critical effect on the fixed interface charge. We could show that these impurities also have an effect on the fast interface state density close to the band edges. This region is not accessable to the conventional measurement techniques. Results for other contaminants, e.g. Pb and Xe, which mainly cause radiation damage are also shown. The experimental results are discussed in the light of theoretical models for MOS interface states.

DLTS-Measurement on MOS Structures

The measurement principle is explained in Figs. 2 and 3. During a 20 µs pulse the MOS capacitor is biased into accumulation to fill all interface traps with majority charge carriers, e.g. in our case electrons. During the pulse interval the bias voltage is adjusted so that the Fermi level in equilibrium is located in a midgap position. The change of the interface charge is monitored by measurement of the MOS capacitance. As indicated in Fig. 3, we use a feedback from the capacitance bridge to the bias power supply to maintain a constant capacitance. The relaxation of the interface charge is then monitored by the bias voltage. The change of the gate voltage required to maintain a constant capacitance appears only across the oxide layer. The interface charge change per unit area $\Delta Q_{ss}(t) = q\Delta N_{ss}$ which is proportional to the interface state density therefore is simply related to the observed gate voltage signal $\Delta V(t)$ by

$$\Delta V(t) = A\Delta Q_{ss}(t)\, C_{0x}, \tag{1}$$

where C_{0x} is the oxide capacitance and A the capacitor metal gate area. It is assumed that during the pulse interval interface states emit the trapped charge by thermal emission [$\sim \exp(-t/\tau_e)$] with time constant

$$1/\tau_e = \sigma_n v_{th} N_C \exp(-E/kT), \tag{2}$$

where σ_n is the capture cross-section and v_{th} the thermal velocity of electrons, N_C the effective density of states in the conduction band, and E the energy depth of the interface state below the conduction band edge. As indicated in Fig. 3, the gate voltage V_G is sampled at two different delay times t_1 and $t_2 = 2t_1$ and the difference signal

$$\Delta V_G = V_G(t_1) - V_G(t_2) \tag{3}$$

is formed in the DLTS measurement. For electron emission from a continuous distribution of interface traps, we obtain for the DLTS signal ΔV_G from (1)–(3)

$$\Delta V_G = A/C_{0x} \int qN_{ss}(E) \cdot [\exp(-t_1/\tau_e) - \exp(-t_2/\tau_e)]\, dE. \tag{4}$$

For a constant or slowly varying capture cross-section and interface state density the integrand is sharply peaked at energy E_0 [6]

$$E_0 = kT \ln(\sigma_n v_{th} N_C t_1 \ln 2) \tag{5}$$

and

$$\Delta U_G = kT \Delta \ln 2 \, N_{ss}(E_0) \, C_{ox}. \tag{6}$$

Thus, the emission signal divided by temperature is directly proportional to the interface state density at energy E_0. The energy interval over which interface traps contribute to the DLTS signal is $\Delta E = kT \ln 2$. Both, the width of the interval ΔE, and its location in energy E_0 increase linearly with temperature. The energy resolution is therefore greatest at low temperatures where the sampled interval is closest to the conduction band and where the interface state density and capture cross-section is expected to vary most rapidly. The larger energy intervals obtained at high temperatures provide enhanced sensitivity for detecting low densities of interface states which are typically found near midgap.

The capture cross-section is obtained from two or more temperature scans taken at different delay time constants t_1 and t_1' by using (5) and noting that the same density of states at a given E_0 is measured at two different temperatures T and T'. The analytical expression for the capture cross-section is

$$\sigma_n = (\ln 2 \, t_1 v_{th} N_C)(t_1'/t_1)^{T'/(T-T')} \tag{7}$$

Equations (5) and (7) are used to analyse the experiment. A comparison of the DLTS-technique with the conventional conductance technique for the measurement of interface state densities is given in Fig. 4. In the conductance technique, the position of the Fermi level is used to probe the energy position of deep levels at the surface. Only those states which are within a few kT in the vicinity of the Fermi level contribute to the measured conductance signal.

The transition of charge carriers which is sensed in the conductance technique is marked by CT in Fig. 4a. Bulk levels are only measured at the cross-over with the Fermi level. This cross-over occurs in a narrow region because of the band bending. The conductance technique is therefore insensitive to bulk states.

The effect of potential fluctuations in the surface is indicated in Fig. 4b. In the conductance technique, the energy resolution is smeared out by the potential fluctuation. In the DLTS-technique, the emission time constant is measured. This time constant is only dependent on the local energy depth under the band edge for pure thermal emission and is independent of the position of the Fermi level. The total number of states in the space charge layer is measured independent of band bending and potential fluctuations. DLTS therefore is very sensitive also to bulk states. However the spectrum of the states is measured as a function of the emission time constant rather than energy. The energy dependence of the number of states and the capture cross-section can only be obtained by a deconvolution of the measured data. The comparison of the various properties is listed in Fig. 4.

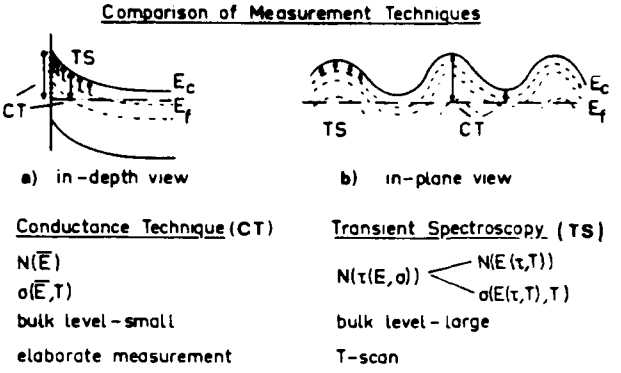

Fig. 4. Comparison of the conductance technique and CC-DLTS technique in the measurement of bulk and interface states in MOS structures

Experiment

The silicon samples (approx. 1 Ohm cm n-type epitaxial material on low resistivity substrate) were implanted before oxidation. The implantation was performed at room temperature at an angle of about 7° with respect to a low-index crystal orientation. The implantation energy was chosen to obtain a projected range of approx. 600 Å according to the LSS table computed by Johnson and Gibbons [10]. The SiO_2 film was grown under standard dry oxidation conditions at 1050 °C to a thickness of 600 to 1200 Å. For the elements under investigation Cs, Pb, Xe it was known from our earlier work where we have performed secondary ion mass spectroscopy SIMS that these imporities pile up at the interface during oxide growth.

For the case of sodium a shallow implantation into the oxide was performed to contaminate the MOS structure intentionally. Sodium can be drifted to and away from the interface at room temperature by applying a dc bias field. A flat band voltage shift from − 6 V to − 34 V was observed after 30 min drift with 10 V dc bias voltage.

The DLTS measurement system has been described elsewhere [4, 8, 9]. The only new feature in CC-DLTS is a feedback loop from the capacitance bridge to the

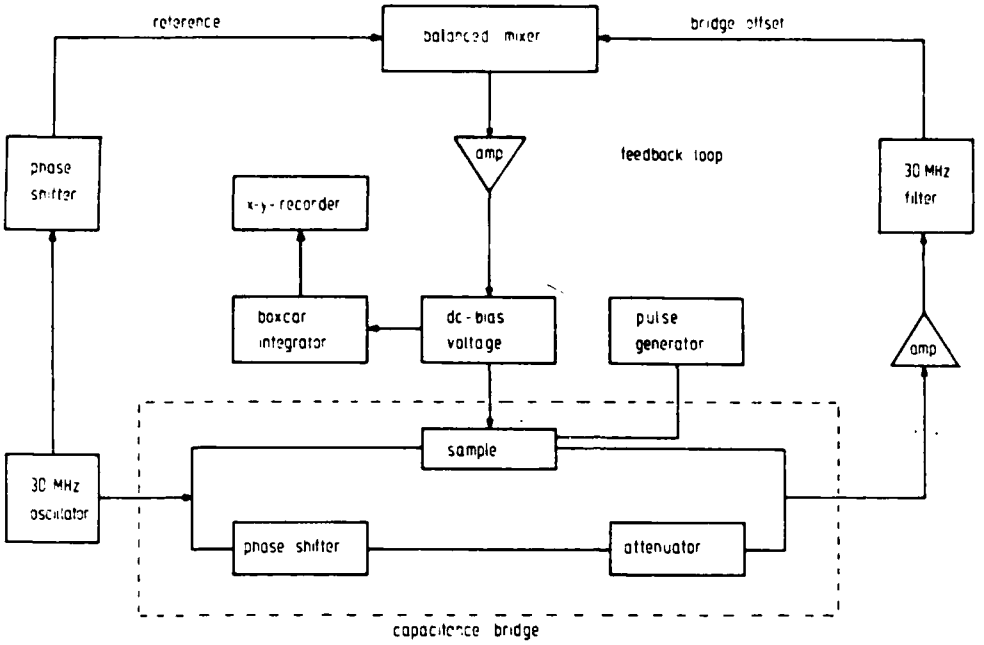

Fig. 5. Block diagram of the apparatus for the CC-DLTS measurement system which is used to analyse interface states

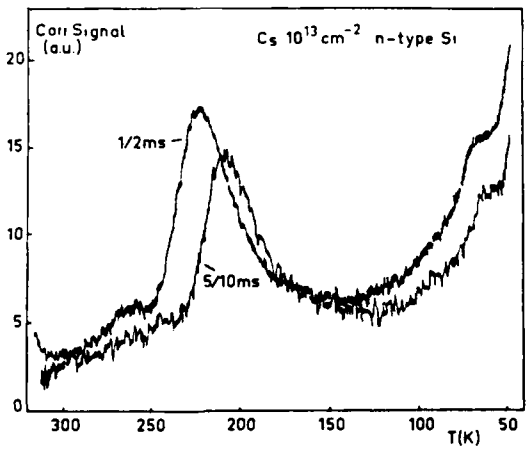

Fig. 6. Temperature scan of the DLTS correlation signal for a cesium contaminated MOS structure. Parameter is the delay time constant used in the DLTS technique

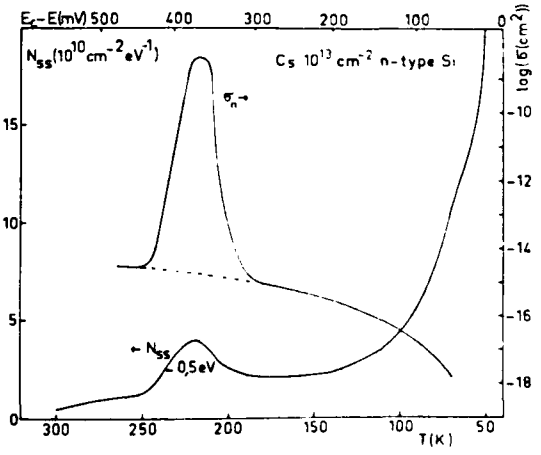

Fig. 7. Density of interface states N_{ss} and capture cross-section σ_n as evaluated from the measurement in Fig. 6 for a cesium contaminated MOS structure

dc voltage supply to maintain a constant capacitance of the MOS structure. The block diagram of the measurement system is shown in Fig. 5.

Results

A typical temperature scan of the DLTS signal for a Cs contaminated sample is shown in Fig. 6. Two temperature scans of the DLTS correlation signal taken with two pairs of sampling delay times 1.2 ms (i.e. 1 and 2 ms) and 5/10 ms were recorded. The cesium dose implanted into the bare silicon before oxidation was 10^{13} cm^{-2}. The shape of the observed signal vs. temperature is quite different to the shape observed in state-of-the-art clean samples [6, 9]. A steep increase of the signal is observed at low temperatures. A strong peak is superimposed at approx. 220 K.

In Fig. 7 the experimental curves of Fig. 6 are evaluated to obtain the density of interface states N_{ss} and the capture cross-section σ_n by using (6) and (7). The values N_{ss} and σ_n are plotted as a function of temperature. An approximate energy scale is obtained by using (5) and the continuous curve for σ_n. This scale is marked at the top of Fig. 7. It should be noted, however, that the peak at 220 K which also appears in the capture cross-section does not fit into the continuous energy scale. The energy position of the peak is evaluated to approx. 0.5 eV because of its high capture cross-section. This peak in the density of interface state at 220 K and the peak in the capture cross-section indicate that this state differs from the continuous background of states.

The background density of states is rather low around 10^{10} cm^{-2} eV^{-1} at high temperatures where states near midgap are observed and increases very steeply at low temperatures where states close to the band edge are observed. The increase at low temperatures and shallow energy depths is much steeper than it was observed in state-of-the-art clean MOS samples. The variation of the capture cross-section for the background of interface states (excluding the peak) is comparable to the observation in clean samples. In the midgap region the capture cross-section is of the order 10^{-15} cm^2. At shallow energy depths $E_0 \sim 0.2$ eV the value of the capture cross-section drops to low values of the order of 10^{-18} cm^2. The capture cross-section seems not to be affected by the cesium contamination. Only the density of states near the band edge is strongly increased.

The same general behavior of the number of interface states is observed after sodium contamination by implantation of a small dose 10^{13} cm^{-2} into the surface. The interface state density observed before drift (A) and after drift (B) of sodium ions away from the interface is shown in Fig. 8. The amount of positive sodium ion charge shifted from the interface to the surface is visible in the flat band voltage shift of the order of 28 V. A strong increase of the number of interface states is again observed when a large number of positive sodium ions is present at the interface. The background of states in the sample was quite high of the order 3×10^{11} cm^{-2} eV^{-1}. Because of the mobility of sodium ions in SiO_2 the density of states could not be measured at high temperatures (greater 150 K) under the bias conditions in the measurement. The observed result for sodium, however, is similar to the case of cesium which is stable up to high temperatures.

A result of lead implantation prior to oxidation is shown in Fig. 9. The density of states and the capture cross-section are shown as a function of the measurement temperature. Note the change in the scale for the

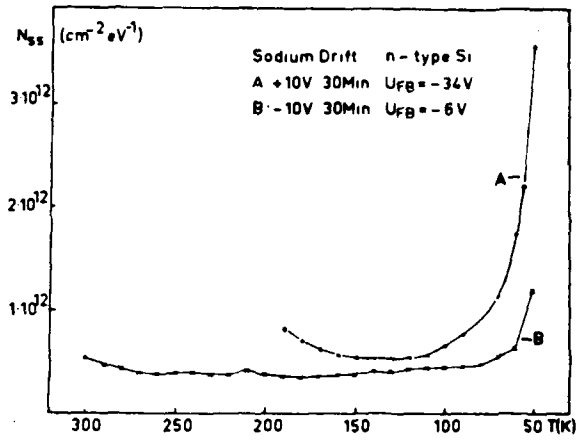

Fig. 8. Density of interface states obtained by the CC-DLTS measurement for a sodium contaminated MOS structure. Sodium ions were drifted to the interface (curve A) and to the metal gate (curve B) by a dc bias stress as shown in the insert. Values of the flat band voltage for each case are also shown in the insert.

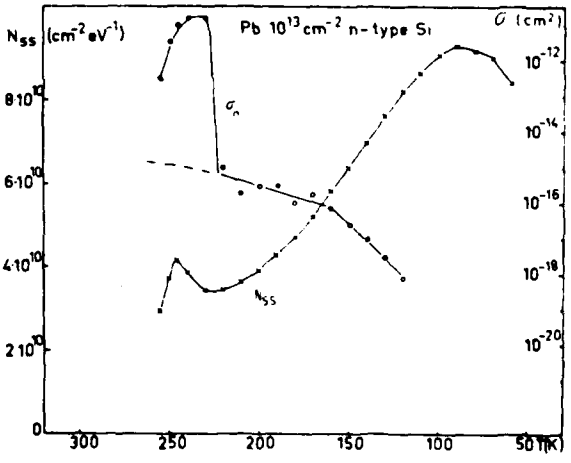

Fig. 9. Density of interface states N_{ss} and capture cross-section σ_n for a MOS structure implanted with lead prior to oxidation.

N_{ss} value in comparison to cesium in Fig. 7! The increase in the number of states at low temperatures is much weaker than for cesium and comparable to the behavior in clean samples. A peak is observed at 240 K which appears in the density of states and the capture cross-section. The background of the capture cross-section for the continuum of interface states shows the same general behavior as was observed for cesium.

In order to study the effect of radiation damage we have implanted a noble gas ion (Xe) prior to oxidation. The sample preparation was not changed. The result is

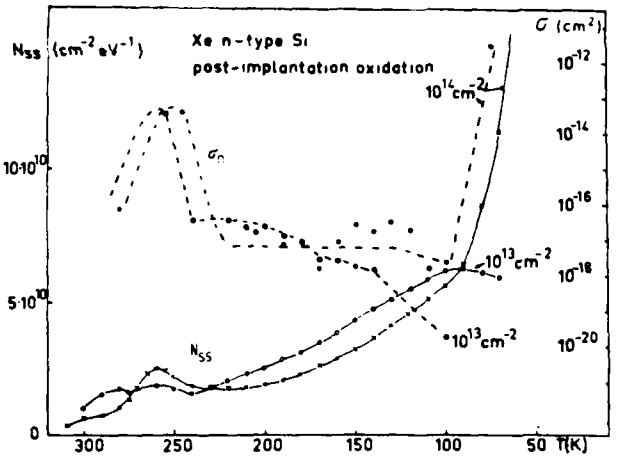

Fig. 10. Density of interface states N_{ss} and capture cross-section σ_n for a MOS structure implanted with Xe-ions prior to oxidation. The implanted doses are shown in the insert

shown in Fig. 10 for two implanted doses of $10^{13}\,cm^{-2}$ and $10^{14}\,cm^{-2}$. The observed result for the dose of $10^{13}\,cm^{-2}$ is similar to the behavior of lead. Peaks are observed in the density of states and capture cross-section around 250 K. The density of states shows a weak increase at low temperatures where states close to the conduction band edge are observed. The capture cross-section decreases to low values. For a high implanted dose $10^{14}\,cm^{-2}$, the density near midgap observed at high temperatures remains low, however, at shallow energies the density of interface states increases very steeply. This behavior seems similar to the behavior of cesium, however, the capture cross-section also shows a steep increase for the high Xe-dose. It is therefore assumed that a new type of level appears at high implanted doses.

Conclusions

The observed results demonstrate that CC-DLTS is very useful to study MOS interface states. The capture cross-section and the number of states are directly observed in a temperature scan of the DLTS correlation signal. The temperature variation can be interpreted as an energy scale. It has been shown earlier [6] that the variation of the capture cross-section is energy dependent. CC-DLTS is especially useful to study the energy region in the vicinity of the band edge. This region was not accessible by other techniques which use the Fermi level to probe the energy position because potential fluctuations smeared out the energy resolution.

Based on the presented CC-DLTS results in comparison with earlier measurements using the conductance technique [11] we arrive at the following conclusions on the influence of impurities in the MOS interface on *n*-type silicon:

- alkali ions increase the number of fast interface states in the energy region close to the conduction band edge
- the density of interface states in the midgap region is very little affected by impurities
- lead ions do not seriously affect the number of interface states up to doses of the order of $10^{13}\,cm^{-2}$ implanted prior to oxidation
- ion implantation prior to oxidation causes a damage level near midgap which appears as a peak in the CC-DLTS temperature scan, independent of the implanted type of ion. Tests with the conductance technique did not show this level. The peak is probably a bulk Si level in the vicinity of the interface because only the CC-DLTS technique is sensitive to bulk levels
- the capture cross-section is energy dependent [6]. The order of magnitude near midgap is $10^{-15}\,cm^2$. The value indicates a neutral trapping center. Near the band edge, the value of the capture cross-section drops to very low values of less than $10^{-18}\,cm^2$
- the emission rate from interface traps is purely temperature activated. This conclusion is a consequence of the observed quantitative agreement with results of the conductance technique
- tunneling to trap centers in the oxide can be excluded because tunneling would be temperature independent. It is therefore not visible in a temperature scan. Tunneling together with a temperature activation would lead to a discrepency with results of the conductance technique because in the evaluation of the CC-DLTS result only temperature activation has been taken into account. However, CC-DLTS and the conductance measurements are in accordance within the measurement error

except in the discrete peaks observed around 240 K, all the interface states are of the same type. The observed variation in density and capture cross-section can be interpreted as a gradual property variation of the same type of state as a function of its energy position. Especially, a transition from one type of state to another can be excluded because two different capture cross-sections are never observed for states at the same energy position. A step in the capture cross-section would be observed if a transition from one type of state to a new type at a given energy is present

- the charge model [12] for the interpretation of interface states seems very unlikely. In the charge model, the free electron is bound to the positive charge center in the oxide similarly as to a donor center in bulk crystals. The charge model cannot account for the

capture cross-section near the band edge. For an attractive center, the capture cross-section for weakly bound electrons is expected to increase rather than to drop to low values as it is observed for bulk donor levels.

Theoretical models which are known at present cannot explain all the observed effects on interface states in MOS structures on *n*-type silicon. Since the number of states is related to the oxide charge, the charge center in the oxide and its coupling to the lattice (multiphonon emission) may dominate the trapping of electrons at the interface. Further experimental details are necessary to develop a theoretical model on firm grounds.

Acknowledgements. The authors express their appreciation to H. Lefevre and F. Pohl for their assistance with the DLTS measurements. The authors profitted from many discussions with Dr. N. M. Johnson from Xerox Palo Alto Research Center. The earlier measurements on state-of-the-art clean MOS structures were performed at Xerox. This cooperation is gratefully acknowledged. The work was partially supported by the US Army Research Office.

References

1. M. Schulz, E. Klausmann, A. Hurrle: CRC Critical Rev. in Sol. State Sci. **5**, No. 3, 319 (1975)
2. A. Hurrle, G. Sixt: Appl. Phys. **8**, 293 (1975)
3. D. V. Lang: J. Appl. Phys. **45**, 3014 and 3023 (1974)
4. H. Lefèvre, M. Schulz: Appl. Phys. **12**, 45 (1977)
5. K. Nagasawa, M. Schulz: Appl. Phys. **8**, 35 (1975)
6. M. Schulz, N. M. Johnson: Sol. State Commun. **25**, 481 (1978); Errata Sol. State Commun. **26**, No. 2, 126i (1978)
7. M. Schulz, N. M. Johnson: Appl. Phys. Lett. **31**, 622 (1977)
8. N. M. Johnson, D. J. Bartelink, M. Schulz: Proc. of Int. Topical Conf. of the Physics of SiO_2 and its Interfaces, to be published
9. N. M. Johnson, M. Schulz: J. Appl. Phys., to be published
10. W. S. Johnson, J. F. Gibbons: "Projected Range Statistics in Semiconductors" (1969)
11. H. Deuling, E. Klausmann, A. Goetzberger: Solid State Electron. **15**, 559 (1972)
12. A. Goetzberger, V. Heine, E. H. Nicollian: Appl. Phys. Lett. **12**, 95 (1968)